Published June 10, 2013

The adhesion protein IgSF9b is coupled to neuroligin 2 via S-SCAM to promote inhibitory synapse development

Jooyeon Woo,[1,2] Seok-Kyu Kwon,[1,2] Jungyong Nam,[1,2] Seungwon Choi,[1,2] Hideto Takahashi,[3] Dilja Krueger,[4] Joohyun Park,[5] Yeunkum Lee,[1,2] Jin Young Bae,[6] Dongmin Lee,[7,8] Jaewon Ko,[9] Hyun Kim,[7,8] Myoung-Hwan Kim,[5] Yong Chul Bae,[6] Sunghoe Chang,[5] Ann Marie Craig,[3] and Eunjoon Kim[1,2]

[1]Center for Synaptic Brain Dysfunctions, Institute for Basic Science (IBS), Daejeon 305-701, South Korea
[2]Department of Biological Sciences, Korea Advanced Institute of Science and Technology (KAIST), Daejeon 305-701, South Korea
[3]Brain Research Centre and Department of Psychiatry, University of British Columbia, Vancouver, British Columbia, Canada
[4]Max Planck Institute of Experimental Medicine, Department of Molecular Neurobiology, D-37075 Göttingen, Germany
[5]Department of Physiology and Biomedical Sciences, Seoul National University College of Medicine, Seoul 110-799, South Korea
[6]Department of Anatomy and Neurobiology, School of Dentistry, Kyungpook National University, Daegu 700-412, South Korea
[7]Department of Anatomy and [8]Division of Brain Korea 21 Project for Biomedical Science, College of Medicine, Korea University, Seoul 136-705, South Korea
[9]Department of Biochemistry, College of Life Science and Biotechnology, Yonsei University, Seoul 120-749, South Korea

Synaptic adhesion molecules regulate diverse aspects of synapse formation and maintenance. Many known synaptic adhesion molecules localize at excitatory synapses, whereas relatively little is known about inhibitory synaptic adhesion molecules. Here we report that IgSF9b is a novel, brain-specific, homophilic adhesion molecule that is strongly expressed in GABAergic interneurons. IgSF9b was preferentially localized at inhibitory synapses in cultured rat hippocampal and cortical interneurons and was required for the development of inhibitory synapses onto interneurons. IgSF9b formed a subsynaptic domain distinct from the $GABA_A$ receptor– and gephyrin-containing domain, as indicated by super-resolution imaging. IgSF9b was linked to neuroligin 2, an inhibitory synaptic adhesion molecule coupled to gephyrin, via the multi-PDZ protein S-SCAM. IgSF9b and neuroligin 2 could reciprocally cluster each other. These results suggest a novel mode of inhibitory synaptic organization in which two subsynaptic domains, one containing IgSF9b for synaptic adhesion and the other containing gephyrin and $GABA_A$ receptors for synaptic transmission, are interconnected through S-SCAM and neuroligin 2.

Introduction

Synaptic adhesion molecules regulate synapse formation, maturation, maintenance, and function (Dalva et al., 2007; Biederer and Stagi, 2008; Südhof, 2008; Brose, 2009; Woo et al., 2009; Johnson-Venkatesh and Umemori, 2010; Shen and Scheiffele, 2010; Tallafuss et al., 2010; Williams et al., 2010; Yuzaki, 2010; Siddiqui and Craig, 2011). Many known synaptic adhesion molecules regulate excitatory synapses, whereas relatively little is known about inhibitory synaptic adhesion molecules, which include neuroligin 2 and slitrk3 (Südhof, 2008; Takahashi et al., 2012).

Neuroligin 2 selectively localizes to inhibitory synapses and regulates the formation and function of inhibitory synapses (Graf et al., 2004; Varoqueaux et al., 2004; Chih et al., 2005; Levinson et al., 2005; Chubykin et al., 2007). Mouse genetic studies have confirmed that neuroligin 2 regulates GABAergic synapse maturation, inhibitory synaptic transmission, neuronal excitability, retinal signal processing, and anxiety-like behaviors (Varoqueaux et al., 2006; Chubykin et al., 2007; Blundell et al., 2009; Gibson et al., 2009; Hoon et al., 2009; Jedlicka et al., 2011; Poulopoulos et al., 2009).

J. Woo, S.-K. Kwon, J. Nam, S. Choi, and H. Takahashi contributed equally to this paper.

Correspondence to Eunjoon Kim: kime@kaist.ac.kr or Ann Marie Craig: acraig@mail.ubc.ca

Abbreviations used in this paper: ANOVA, analysis of variance; DIV, day in vitro; IgSF, immunoglobulin superfamily; mEPSC, miniature excitatory postsynaptic current; mIPSC, miniature inhibitory postsynaptic current; PSD, postsynaptic density; STORM, stochastic optical reconstruction microscopy; VGAT, vesicular GABA transporter.

Supplemental Material can be found at:
http://jcb.rupress.org/content/suppl/2013/06/10/jcb.201209132.DC1.html
Original image data can be found at:
http://jcb-dataviewer.rupress.org/jcb/browse/6317

The Rockefeller University Press $30.00
J. Cell Biol. Vol. 201 No. 6 929–944
www.jcb.org/cgi/doi/10.1083/jcb.201209132

Published June 10, 2013

Neuroligin 2 interacts extracellularly with presynaptic neurexins and triggers inhibitory presynaptic differentiation in contacting axons (Graf et al., 2004; Chih et al., 2005; Levinson et al., 2005). The cytoplasmic region of neuroligin 2 contains two motifs involved in protein–protein interactions. The one located in the middle of the cytoplasmic region directly interacts with gephyrin (Poulopoulos et al., 2009), a major inhibitory postsynaptic scaffold (Fritschy et al., 2008; Fritschy et al., 2012). This interaction is thought to lead to a close apposition of neuroligin 2 with various gephyrin-associated proteins, including $GABA_A$ receptors and glycine receptors (Fritschy et al., 2008, 2012). Notably, neuroligin 2, but not other neuroligins, selectively activates collybistin, a RhoGEF for Cdc42 that binds both gephyrin and the plasma membrane and, thus, leads to the stable tethering of gephyrin to the inhibitory synaptic membrane (Poulopoulos et al., 2009).

The C terminus of neuroligin 2 contains a PDZ-binding motif that interacts with PSD-95 (Irie et al., 1997) and S-SCAM (also known as MAGI-2; Sumita et al., 2007), two postsynaptic scaffolding proteins equipped with multiple domains for protein–protein interactions including PDZ and GK domains (Hirao et al., 1998; Sheng and Kim, 2011). The functional significance of the interaction between neuroligin 2 and PSD-95 remains unclear because these two proteins mainly localize at inhibitory and excitatory synapses, respectively (Sumita et al., 2007; Sheng and Kim, 2011).

S-SCAM, however, distributes to both excitatory and inhibitory synapses, with ∼35% of clusters being detected at inhibitory synapses, which is dissimilar to PSD-95 (Sumita et al., 2007). This suggests the possibility that S-SCAM, together with its binding partner neuroligin 2, contributes to the organization of inhibitory synapses. Moreover, highlighting the clinical importance of S-SCAM, chromosomal mutations in the human S-SCAM/MAGI-2 gene have been associated with infantile spasm (also known as West syndrome), an epileptic disorder characterized by seizure, distinct EEG (termed hypsarrhythmia), and intellectual disability (or mental retardation; Marshall et al., 2008).

Dasm1 (also known as IgSF9; Doudney et al., 2002) is an Ig superfamily (IgSF) adhesion molecule reported to regulate dendritic arborization and excitatory synaptic maturation in hippocampal neurons by knockdown and dominant-negative approaches (Shi et al., 2004a,b), although a more recent study using mice deficient of Dasm1/IgSF9 showed that dendritic arborization in hippocampal neurons from these animals is normal (Mishra et al., 2008). A *Drosophila* homologue of Dasm1 known as Turtle regulates dendritic branching and self-avoidance as well as axonal path finding and self-avoidance (Doudney et al., 2002; Al-Anzi and Wyman, 2009; Ferguson et al., 2009; Long et al., 2009). Dasm1 in mammals has a close relative termed IgSF9b, which shares a similar domain structure with Dasm1; five Ig domains, two fibronectin III (FNIII) domains, one transmembrane domain, and a C-terminal PDZ-binding motif. Importantly, IgSF9b has recently been associated with major depressive disorder (Shyn et al., 2011), but the physiological function of IgSF9b remains unexplored.

In the present study, we found that IgSF9b is selectively expressed in the brain, strongly expressed in GABAergic interneurons, preferentially localized at inhibitory synapses, and required for the development of inhibitory synapses onto interneuronal dendrites. Intriguingly, IgSF9b is localized to a subsynaptic domain distinct from a $GABA_A$ receptor/gephyrin-containing subsynaptic domain. IgSF9b is linked, via the multi-PDZ protein S-SCAM, to neuroligin 2, which is coupled to gephyrin. These results suggest a novel mode of inhibitory synaptic organization, with detailed molecular mechanisms, where two subsynaptic domains with differential functions, i.e., adhesion and transmission, may act synergistically to develop inhibitory synapses.

Results

IgSF9b is abundantly expressed in GABAergic interneurons

To understand the function of IgSF9b, a structural homologue of Dasm1 (Figs. 1 A and S1 A), we first generated two different polyclonal antibodies for IgSF9b using two largely independent C-terminal regions of IgSF9b as antigens, where they share minimal amino acid sequence identities with Dasm1/IgSF9 (1593 and 1913; Fig. S1, A and B). These two antibodies revealed essentially identical immunostaining patterns in cultured hippocampal neurons (Fig. S1 C). In addition, a commercially available IgSF9b antibody (HPA010802), raised against another independent region (Fig. S1 B), revealed a similar distribution pattern (Fig. S1 D). The similar distribution patterns of IgSF9b revealed by independent antibodies suggest that the observed IgSF9b signals are authentic.

In cultured hippocampal neurons, IgSF9b signals were detected in punctate clusters in the cell body and dendrite regions of GABAergic interneurons that are positive for the GABA synthetic enzyme glutamic acid decarboxylase GAD67. The majority of GABAergic neurons (∼80%) exhibited punctate IgSF9b immunofluorescence (n = 15). In contrast, relatively weak signals were detected in some but not all GAD67-negative pyramidal neurons (Fig. 1 B). These results indicate that IgSF9b is more abundant in GABAergic interneurons than in pyramidal neurons.

IgSF9b is mainly present at inhibitory synapses

IgSF9b clusters colocalized with the vesicular GABA transporter (VGAT; an inhibitory presynaptic protein) in pyramidal neurons (Fig. 1 C) and in interneurons (Fig. 1 D). IgSF9b also colocalized with gephyrin, an inhibitory postsynaptic protein, and the α1 subunit of $GABA_A$ receptors in interneurons (Fig. 1, E and F). In contrast, IgSF9b minimally colocalized with the vesicular glutamate transporter vGlut1 and Shank (excitatory pre- and postsynaptic proteins, respectively) in interneurons (Fig. 1 G). In quantitative analysis, ∼78% of IgSF9b puncta colocalized with GAD67 (n = 20).

In cultured cortical neurons, IgSF9b displayed distribution patterns similar to those observed in hippocampal neurons, being more abundant in GAD65-positive GABAergic interneurons

Published June 10, 2013

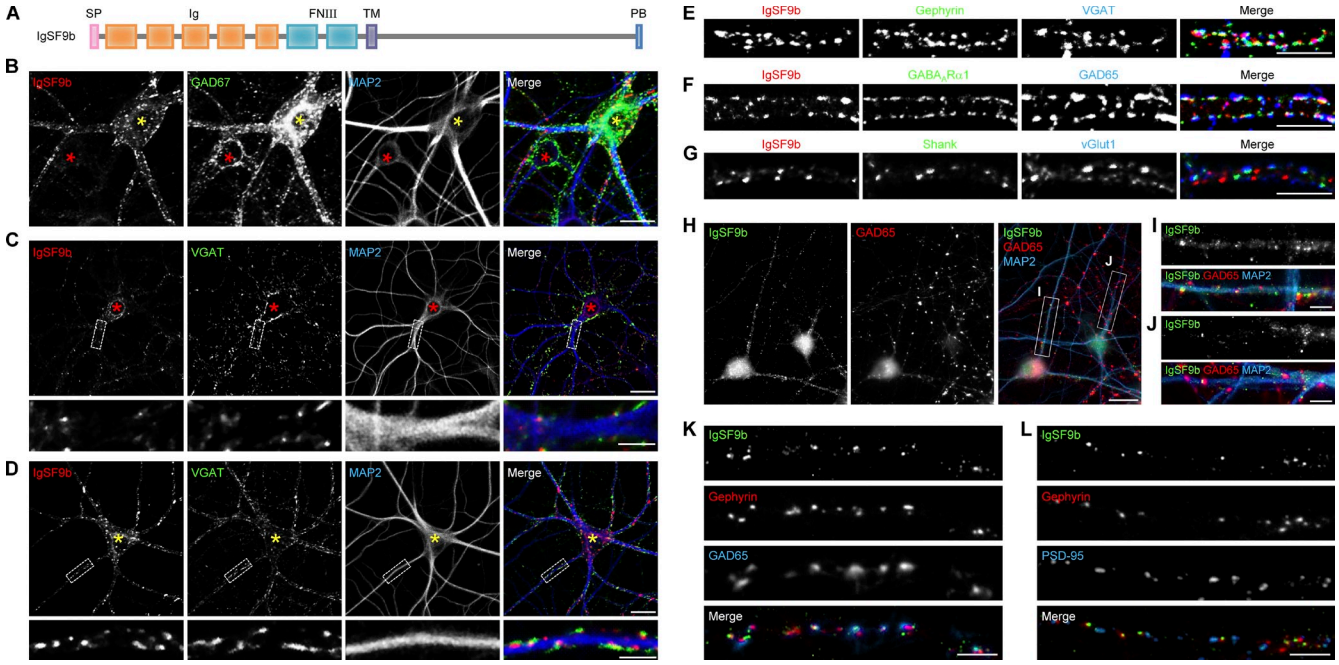

Figure 1. **IgSF9b is abundant in GABAergic interneurons and mainly present at inhibitory synapses.** (A) Domain structure of IgSF9b. SP, signal peptide; Ig, immunoglobulin domain; FNIII, fibronectin type III domain; TM, transmembrane domain; PB, PDZ domain-binding motif. (B) IgSF9b signals are more abundant in interneurons than in pyramidal neurons. Cultured hippocampal neurons (DIV 28, a stage after IgSF9b reaches a plateau of its expression) were labeled by triple immunofluorescence staining for IgSF9b, GAD67, and MAP2. Yellow and red asterisks indicate cell bodies of GAD67-positive interneurons and GAD67-negative pyramidal neurons, respectively. (C and D) IgSF9b colocalizes with VGAT (an inhibitory presynaptic protein) both in pyramidal neurons (C) and in interneurons (D). The bottom images are enlarged views of the boxed regions. (E–G) IgSF9b colocalizes with gephyrin (E) and the α1 subunit of $GABA_A$ receptors (F) at VGAT- or GAD65 (an inhibitory presynaptic protein)-positive inhibitory synapses, but not with vGlut1 (an excitatory presynaptic protein)- or Shank (an excitatory postsynaptic protein)-positive excitatory synapses (G) in interneurons. (H–J) In cultured cortical neurons at DIV 28, IgSF9b is more abundantly expressed in GAD65-positive interneurons than in GAD65-negative pyramidal neurons, and colocalizes with GAD65-positive inhibitory synapses (I and J). (K and L) IgSF9b colocalizes with gephyrin and GAD65 but not with PSD-95 in dendrites of cortical interneurons. Bars: (B) 20 µm; (C and D, top rows) 20 µm; (C and D, bottom rows) 5 µm; (E–G) 10 µm; (H) 20 µm; (I–L) 5 µm.

(Fig. 1 H), and being mainly present at inhibitory synapses (Fig. 1, I and J). IgSF9b colocalized with gephyrin but not with PSD-95 in interneurons (Fig. 1, K and L). These results indicate that IgSF9b mainly localizes to inhibitory synapses. Whereas IgSF9b signals were strong in dissociated neurons, IgSF9b immunofluorescence in rat brain slices could not be easily detected, perhaps because of antigen masking by tight association of IgSF9b with synapses (see the paragraph below describing Fig. 2 F).

Expression patterns of IgSF9b

We first examined distribution patterns of IgSF9b mRNAs in the rat brain by in situ hybridization. IgSF9b mRNAs were detected in various rat brain regions including cortex, hippocampus, thalamus, olfactory bulb, and cerebellum (Fig. 2 A). In addition to the longest splice variant of IgSF9b, two shorter variants may be expressed based on the database (Fig. S2 A). However, in situ probes directed to the three different mRNA regions revealed similar expression patterns in the mouse brain (Fig. S2 B), which suggests that the two shorter variants, if expressed, are unlikely to be expressed in different cell types.

In Western blot analysis, IgSF9b proteins (~190 kD) were mainly detected in the brain but not in other tissues (Fig. 2 B). IgSF9b proteins were detected in brain regions including cortex, hippocampus, cerebellum, and striatum, as revealed by immunoblot analysis (Fig. 2 C), similar to the in situ hybridization results. Levels of IgSF9b proteins increased gradually during the first 3 wk of postnatal rat brain development (Fig. 2 D). Similar increases were also observed in dissociated hippocampal neurons (Fig. S2, C–E). IgSF9b was more abundant in synaptic fractions, including crude synaptosomes (P2) and synaptic plasma membranes (LP1), relative to other subcellular fractions. A similar synaptic abundance could also be observed for known inhibitory synaptic proteins including neuroligin 2, gephyrin, and $GABA_A$ receptor subunits (α1 and γ2; Fig. 2 E).

Within crude synaptosomes, IgSF9b was highly enriched in postsynaptic density (PSD) fractions, being detected in PSD III, the most detergent-resistant PSD fraction (Fig. 2 F). This extent of PSD enrichment is comparable to that of PSD-95, an excitatory postsynaptic scaffolding protein tightly associated with the PSD. Notably, the γ2 subunit of $GABA_A$ receptors was also highly detected in PSD III, whereas neuroligin 2 and the α1 subunit of $GABA_A$ receptors were enriched up to PSD II. These results suggest that IgSF9b, together with the γ2 subunit of $GABA_A$ receptors, is tightly associated with inhibitory synapses.

Because IgSF9b is a novel membrane protein, we examined glycosylation patterns of IgSF9b. Neuraminidase significantly reduced the size of IgSF9b, whereas *O*-glycosidase combined with neuraminidase did not further reduce the size of IgSF9b (Fig. 2 G), indicating that IgSF9b is mainly modified by sialylation, but not by *O*-glycosylation. PNGase F slightly reduced the size of IgSF9b, which indicates that IgSF9b is moderately *N*-glycosylated.

Published June 10, 2013

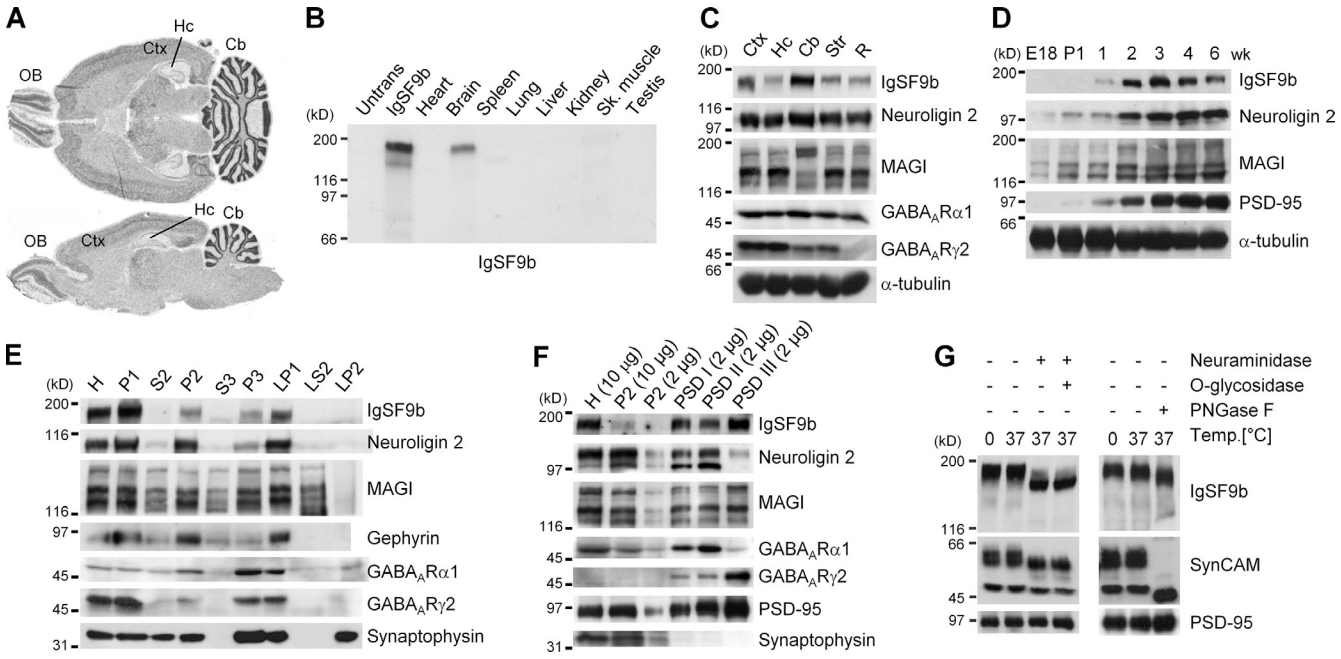

Figure 2. **Expression patterns of IgSF9b.** (A) Distribution of IgSF9b mRNA in rat brain sections revealed by in situ hybridization. OB, olfactory bulb; Ctx, cortex; Hc, hippocampus; Cb, cerebellum. (B) IgSF9b protein is mainly expressed in the rat brain, as revealed by immunoblot analysis. Untransfected (Untrans) and IgSF9b-transfected (IgSF9b) HEK cell lysates were used as controls. Sk. muscle, skeletal muscle. (C) Widespread distribution of IgSF9b proteins in rat brain regions. Str, striatum; R, the rest of the brain regions. (D) IgSF9b protein levels gradually increase during postnatal rat brain development and reach a peak at 3 wk. Whole brain homogenates were used. E, embryonic day; P, postnatal day. (E) IgSF9b is more abundant in synaptic rat brain fractions including crude synaptosomes (P2) and synaptic membranes (LP1), relative to other subcellular fractions. Equal amounts of proteins (10 µg) were loaded into each lane. H, homogenates; S2, supernatant after P2 precipitation; S3, cytosol; P3, light membranes; LS2, synaptosomal cytosol; LP2, synaptic vesicle-enriched fraction. (F) Enrichment of IgSF9b in PSD fractions within crude synaptosomes. PSD fractions were prepared by extraction of synaptosomes with Triton X-100 once (PSD I), twice (PSD II), or with Triton X-100 and sarcosyl (PSD III). The amounts of proteins loaded are indicated. (G) IgSF9b is modified strongly by sialylation, moderately by *N*-glycosylation, and minimally by *O*-glycosylation. The crude synaptosomal (P2) fraction of adult rat brains was treated with neuraminidase (for sialylation), neuraminidase + *O*-glycosidase (for sialylation + *O*-glycosylation), and PNGase F (for *N*-glycosylation). SynCAM and PSD-95 were used as positive and negative controls, respectively.

IgSF9b mediates homophilic adhesion

IgSF9b contains adhesion domains (Ig and FNIII) in the extracellular region, and turtle, a *Drosophila* homologue of IgSF9b and Dasm1/IgSF9, mediates homophilic adhesion (Ferguson et al., 2009). To test whether IgSF9b mediates homophilic adhesion, we incubated HEK293T cells expressing IgSF9b with recombinant, soluble IgSF9b protein (the ectodomain of IgSF9b fused to human Fc; IgSF9b-Ecto-Fc). IgSF9b-Ecto-Fc bound to IgSF9b on HEK293T cells but not to other adhesion molecules, including Dasm1/IgSF9 (Fig. 3 A), which suggests that IgSF9b mediates homophilic adhesion.

In addition, IgSF9b expressed in HEK293T cells accumulated at sites of cell–cell contacts (Fig. 3 B). Moreover, IgSF9b on HEK293T cells induced accumulation of IgSF9b on contacting neurites of cocultured neurons, whereas control HEK293T cells expressing EGFP alone did not (Fig. 3 C). Similar results were obtained in GABAergic interneurons and pyramidal neurons (Fig. S3, A and B). These results suggest that IgSF9b mediates homophilic cell adhesion.

IgSF9b is not sufficient to induce synapse formation

Given that IgSF9b is a homophilic adhesion molecule enriched at inhibitory synapses, IgSF9b might function as a synaptic organizer that induces protein clustering in contacting axons and dendrites. In the coculture (or mixed culture) assay, an assay commonly used to test the capabilities of adhesion molecules to trigger synapse formation (Scheiffele et al., 2000; Biederer and Scheiffele, 2007), IgSF9b-expressing HEK293T cells did not induce clustering of the presynaptic protein synapsin I, VGAT, or vGlut1 in contacting axons of cocultured hippocampal neurons (Fig. 3, D and E; and Fig. S3, C–F). Similarly, IgSF9b did not induce clustering of postsynaptic proteins (gephyrin and PSD-95) in contacting dendrites of GABAergic interneurons and pyramidal neurons (Fig. 3, F–I; and Fig. S3, G and H). These results suggest that IgSF9b lacks the activity to induce synaptic protein clustering in contacting axons and dendrites.

Postsynaptic IgSF9b knockdown reduces the number of VGAT-positive gephyrin clusters in interneurons

Although IgSF9b alone is not sufficient to trigger synapse formation, IgSF9b may still regulate inhibitory synaptic functions. To this end, we generated an IgSF9b shRNA knockdown construct (sh-IgSF9b) coexpressing EGFP, along with a mutant sh-IgSF9b construct that lacks knockdown activity (sh-IgSF9b*) as a control. When expressed in HEK293T cells and cultured hippocampal neurons (day in vitro [DIV] 15–20), sh-IgSF9b substantially reduced IgSF9b expression by ∼70% in cultured neurons (Fig. S4, A–D). We expressed sh-IgSF9b or control

Published June 10, 2013

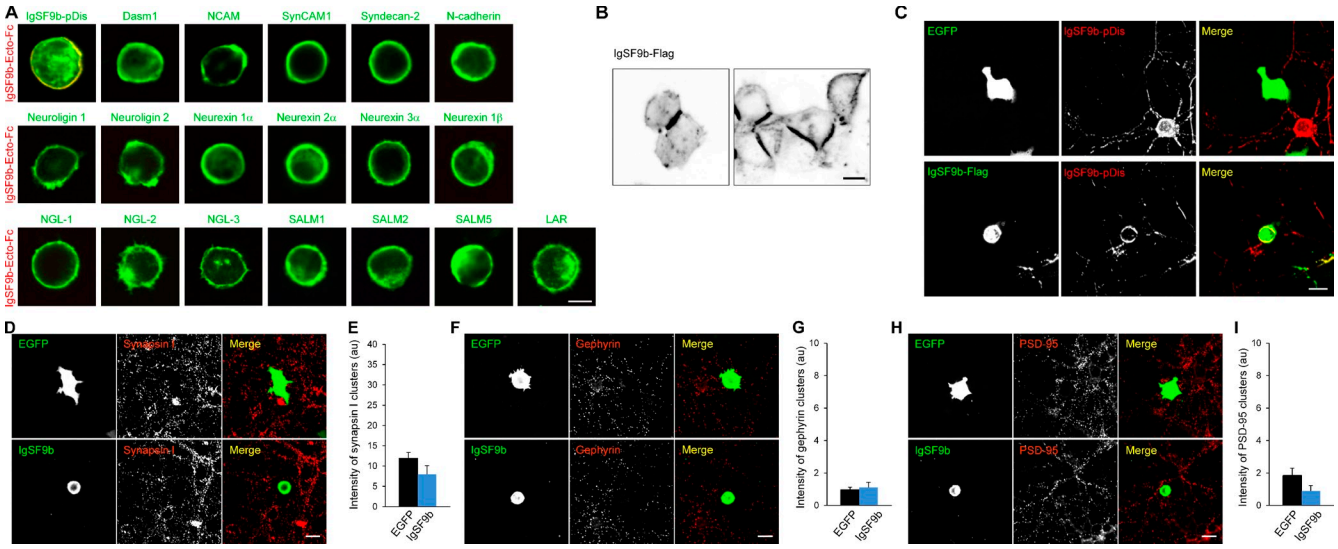

Figure 3. **IgSF9b mediates homophilic adhesion but is not sufficient to induce synapse formation.** (A) Homophilic adhesion by IgSF9b. HEK293T expressing IgSF9b-pDis (ectodomain of IgSF9b in pDisplay vector), or other synaptic adhesion molecules, were incubated with IgSF9b-Ecto-Fc, followed by staining for Fc and the expressed adhesion molecules. (B) IgSF9b accumulates at sites of cell–cell contacts. HEK293T cells were transfected with C-terminally Flag-tagged IgSF9b that lacks the cytosolic region (IgSF9b-Flag), and stained for Flag. (C) IgSF9b-expressing HEK293T cells induce clustering of IgSF9b in contacting neurites of cocultured neurons. HEK293T cells expressing IgSF9b-Flag were cocultured with hippocampal neurons transfected with IgSF9b-pDis (detected with anti-HA). (D–I) IgSF9b-expressing HEK293T cells do not induce clustering of synapsin I (D), gephyrin (F), or PSD-95 (H) in contacting axons or dendrites. HEK293T cells transfected with IgSF9b-pDis, or EGFP alone (negative control), were cocultured with hippocampal neurons (DIV 9–12) and stained for the indicated synaptic proteins. (E, G, and I) Quantification of integrated intensities of the synaptic proteins on HEK293T cells normalized to the cell area. au, arbitrary units. Error bars indicate mean ± SEM. n = 15 (EGFP) and 16 (IgSF9b) for synapsin I, 14 and 16 for gephyrin, and 15 and 18 for PSD-95. A Student's t test was used. Bars: (A and B) 10 µm; (C) 20 µm; (D, F, and H) 20 µm.

constructs in a small fraction of neurons in culture and assessed synapses made onto the somatodendritic domain of these neurons. In this system, the presynaptic inputs arise mainly from surrounding untransfected axons, thus knockdown will reveal roles of postsynaptic IgSF9b.

sh-IgSF9b expressed in interneurons caused a small but significant decrease in the number of inhibitory synapses, defined by VGAT-positive gephyrin clusters, compared with empty shRNA vector (sh-vec; negative control; Fig. 4, A and B). In contrast, sh-IgSF9b* had no effect on inhibitory synapse number in interneurons. IgSF9b knockdown had no effect on excitatory synapse number (vGlut1-positive PSD-95 clusters) in interneurons (Fig. 4, C and D). In pyramidal neurons, where weaker IgSF9b expression is observed, sh-IgSF9b caused a tendency

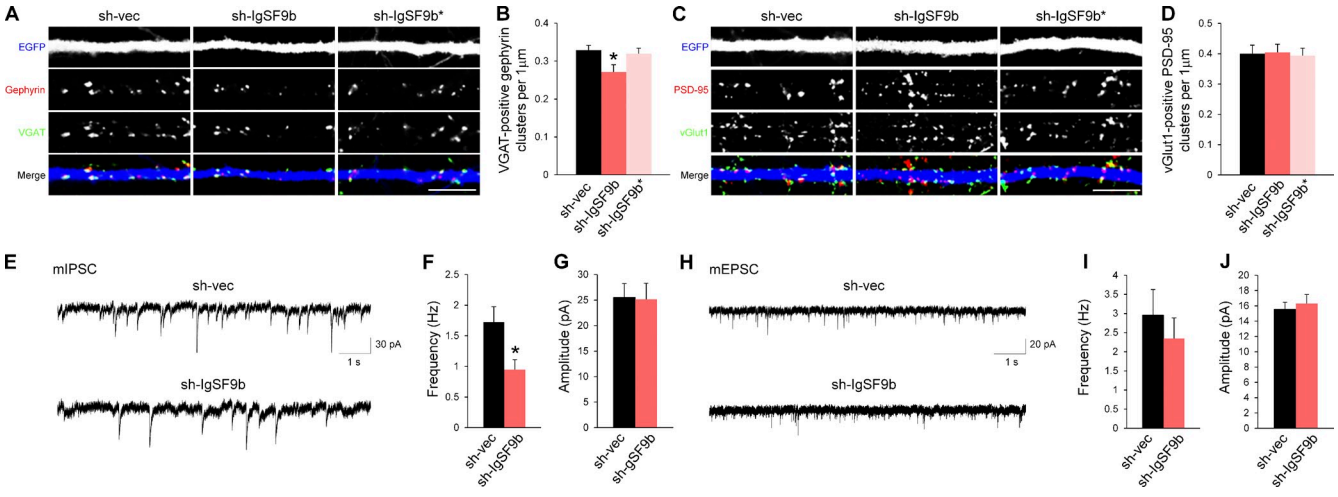

Figure 4. **IgSF9b knockdown reduces the number of VGAT-positive gephyrin clusters and the frequency of inhibitory synaptic transmission in interneurons.** (A) IgSF9b knockdown reduces the number of inhibitory synapses (VGAT-positive gephyrin) in interneurons. Cultured hippocampal neurons expressing sh-vec, sh-IgSF9b, or sh-IgSF9b* (DIV 15–20) were triply stained for EGFP, gephyrin, and VGAT. Bar, 10 µm. (B) Quantification of the results from A. n = 22; *, $P < 0.05$, ANOVA and Tukey's multiple comparison test. (C) IgSF9b knockdown has no effect on the number of excitatory synapses (vGlut1-positive PSD-95) in interneurons. Bar, 10 µm. (D) Quantification of the results from C. n = 19, ANOVA and Tukey's multiple comparison test. (E–G) IgSF9b knockdown reduces the frequency (F) but not amplitude (G) of mIPSCs in interneurons. Sample traces of mIPSCs are shown in E. n = 22 for sh-vec and 20 for sh-IgSF9b; *, $P < 0.05$; Student's t test. (H–J) IgSF9b knockdown has no effect on the frequency (I) or amplitude (J) of mEPSCs in interneurons. n = 22 for sh-vec and 20 for sh-IgSF9b, Student's t test. Error bars indicate mean ± SEM.

Published June 10, 2013

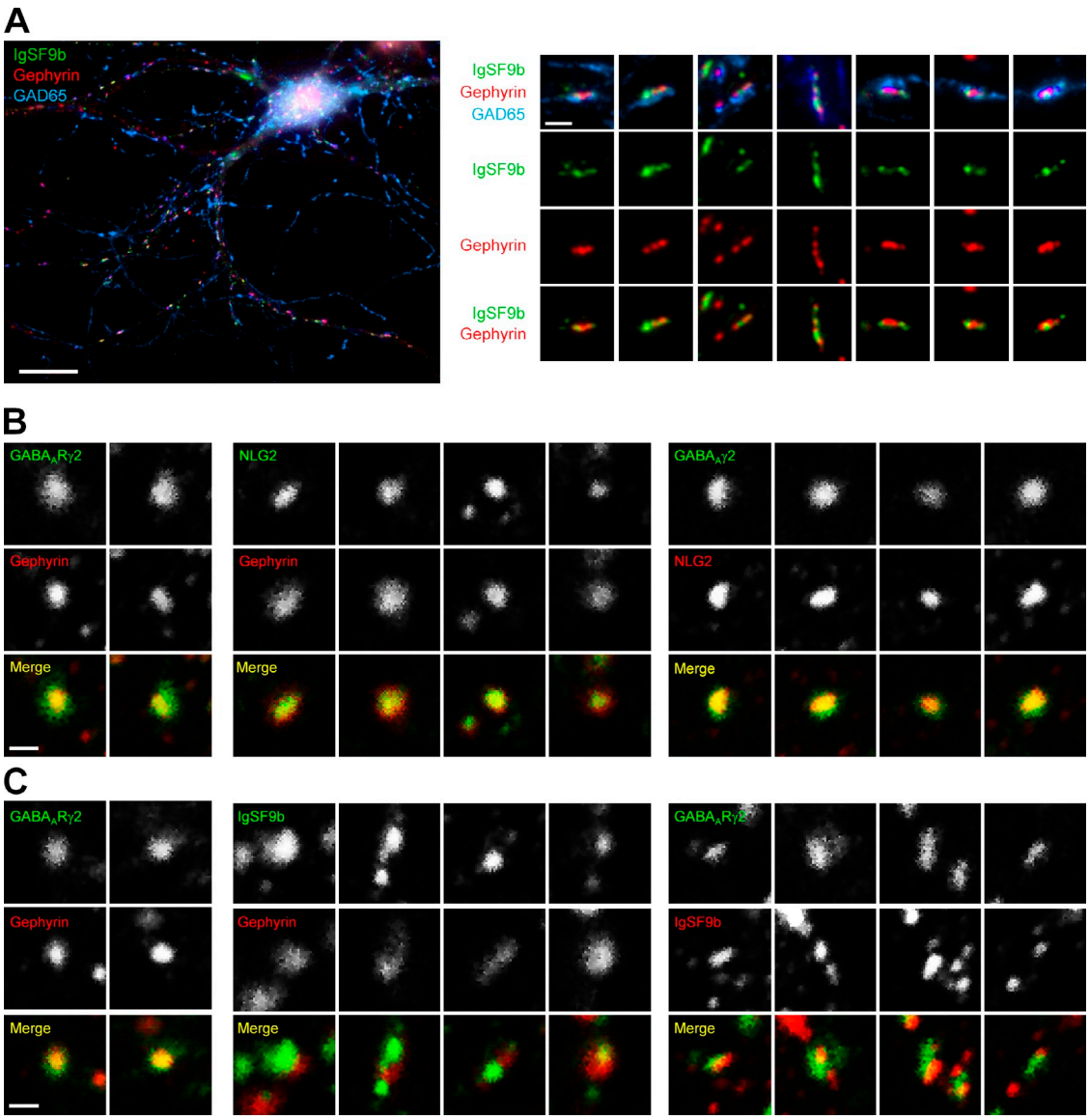

Figure 5. **Gephyrin colocalizes with neuroligin 2 and the γ2 subunit of $GABA_A$ receptors, whereas IgSF9b displays close but minimally overlapping localization with gephyrin or the γ2 subunit of $GABA_A$ receptors.** (A) In normal-resolution immunofluorescence imaging, IgSF9b and gephyrin show closely associated but distinct distribution patterns at GAD65-positive inhibitory synapses. Cultured hippocampal neurons (DIV 21) were triply stained for IgSF9b, gephyrin, and GAD65. (B and C) Cultured hippocampal neurons (DIV 21) were visualized by the combinations of double staining indicated and normal (non-STORM) light microscopy. Bars: (A, left) 20 µm; (A, right) 2 µm; (B and C) 1 µm.

to reduce inhibitory synapse number, although it did not reach statistical significance (Fig. S4, E–H). These results suggest that postsynaptic IgSF9b is important for the development of inhibitory synapses in interneurons, which is consistent with the finding that IgSF9b is abundantly expressed in interneurons and is mainly present at inhibitory synapses.

Postsynaptic IgSF9b knockdown reduces inhibitory synaptic transmission in interneurons

We next evaluated whether IgSF9b knockdown affects inhibitory synaptic transmission. IgSF9b knockdown reduced the frequency of miniature inhibitory postsynaptic currents (mIPSCs) in interneurons, whereas sh-vec had no effect (Fig. 4, E and F). The amplitude of mIPSCs, however, was unaffected by sh-IgSF9b (Fig. 4, E and G). Contrary to mIPSCs, sh-IgSF9b had no effect on miniature excitatory postsynaptic currents (mEPSCs) in both frequency and amplitude (Fig. 4, H–J). Therefore, postsynaptic IgSF9b is required for normal frequency of inhibitory transmission in interneurons, which is consistent with its role in controlling inhibitory synapse number.

IgSF9b and gephyrin/$GABA_A$ receptors display distinct subsynaptic distributions

While searching for mechanisms underlying IgSF9b-dependent inhibitory synapse development, we turned to the observation that IgSF9b and gephyrin often display close but partially nonoverlapping localization at GAD65-positive inhibitory synapses in cultured hippocampal neurons (Fig. 5 A). We thus tested more systematically various combinations of double staining

Published June 10, 2013

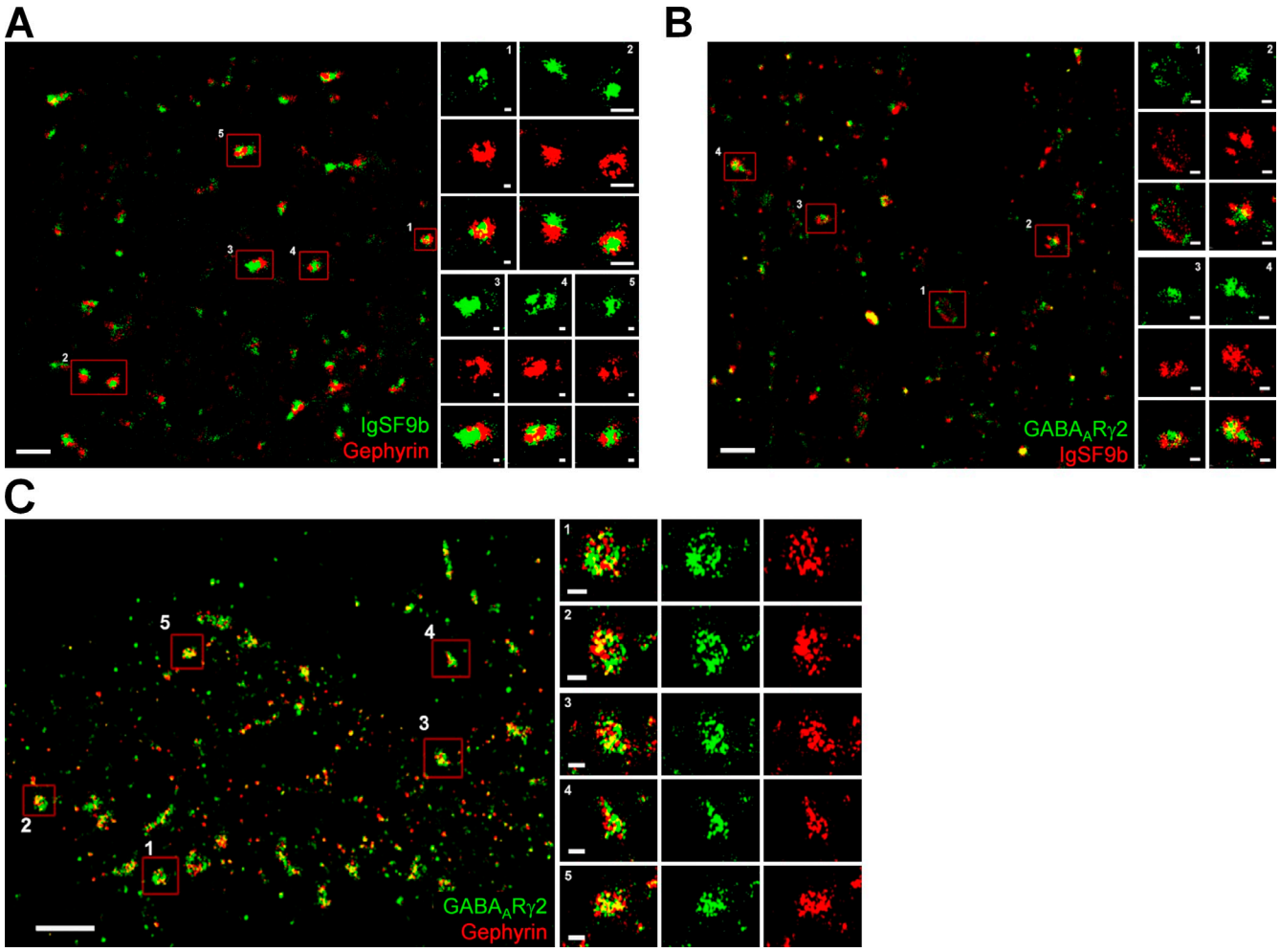

Figure 6. **IgSF9b and gephyrin/GABA$_A$ receptors localize to distinct subsynaptic domains at inhibitory synapses.** (A and B) In super-resolution imaging, IgSF9b and gephyrin, or IgSF9b and the γ2 subunit of GABA$_A$ receptors, show closely associated but minimally overlapping distribution patterns. Cultured hippocampal neurons at DIV 19–20 were used. (C) In super-resolution imaging, gephyrin and the γ2 subunit of GABA$_A$ receptors show substantially overlapping distribution patterns. Cultured hippocampal neurons at DIV 19–20 were used. Bars: (A and B, left) 1,000 nm; (A and B, insets) 100 nm; (C, left) 2,000 nm; (C, inset) 250 nm.

of inhibitory synaptic proteins. Gephyrin, the γ2 subunit of GABA$_A$ receptors, and neuroligin 2 in pairwise combinations showed substantial overlap (Fig. 5 B). In contrast, IgSF9b often minimally overlapped or formed clusters adjacent but nonoverlapping with gephyrin or the γ2 subunit of GABA$_A$ receptors (Fig. 5 C).

To further explore this at a higher resolution, we used super-resolution immunofluorescence imaging using the two-color stochastic optical reconstruction microscopy (STORM) method, which provides a resolution up to 10 times higher than that of regular immunofluorescence imaging and has been successful in revealing subsynaptic localization of synaptic proteins (Bates et al., 2007; Dani et al., 2010). This approach revealed that IgSF9b and gephyrin localize to distinct subsynaptic domains at inhibitory synapses in cultured hippocampal neurons (Fig. 6 A). Similarly, IgSF9b and the γ2 subunit of GABA$_A$ receptors showed distinct distribution patterns at inhibitory synapses (Fig. 6 B). In contrast, gephyrin and the γ2 subunit of GABA$_A$ receptors showed substantially overlapping distribution patterns (Fig. 6 C).

Because gephyrin and the γ2 subunit of GABA$_A$ receptors are considered to be core components of the inhibitory synapse (Fritschy et al., 2008; Luscher et al., 2011; Fritschy et al., 2012), these results suggest that IgSF9b forms an inhibitory subsynaptic domain that is intimately associated with, but distinct from, the core complex containing GABA$_A$ receptors and gephyrin.

IgSF9b interacts with S-SCAM at inhibitory synapses

The close apposition between IgSF9b- and GABA$_A$ receptor/gephyrin-containing inhibitory subsynaptic domains suggests that there might be a molecular mechanism linking the two domains. To this end, we searched for proteins that interact with IgSF9b.

In a yeast two-hybrid screen with the IgSF9b C terminus (last 75 aa residues), which contains a PDZ domain–binding motif, we identified MAGI-1 (human), a member of the S-SCAM/MAGI family (Hirao et al., 1998), as a novel binding partner of IgSF9b. Because MAGI-1 has been reported to be absent from inhibitory synapses (Sumita et al., 2007), we focused on S-SCAM

Published June 10, 2013

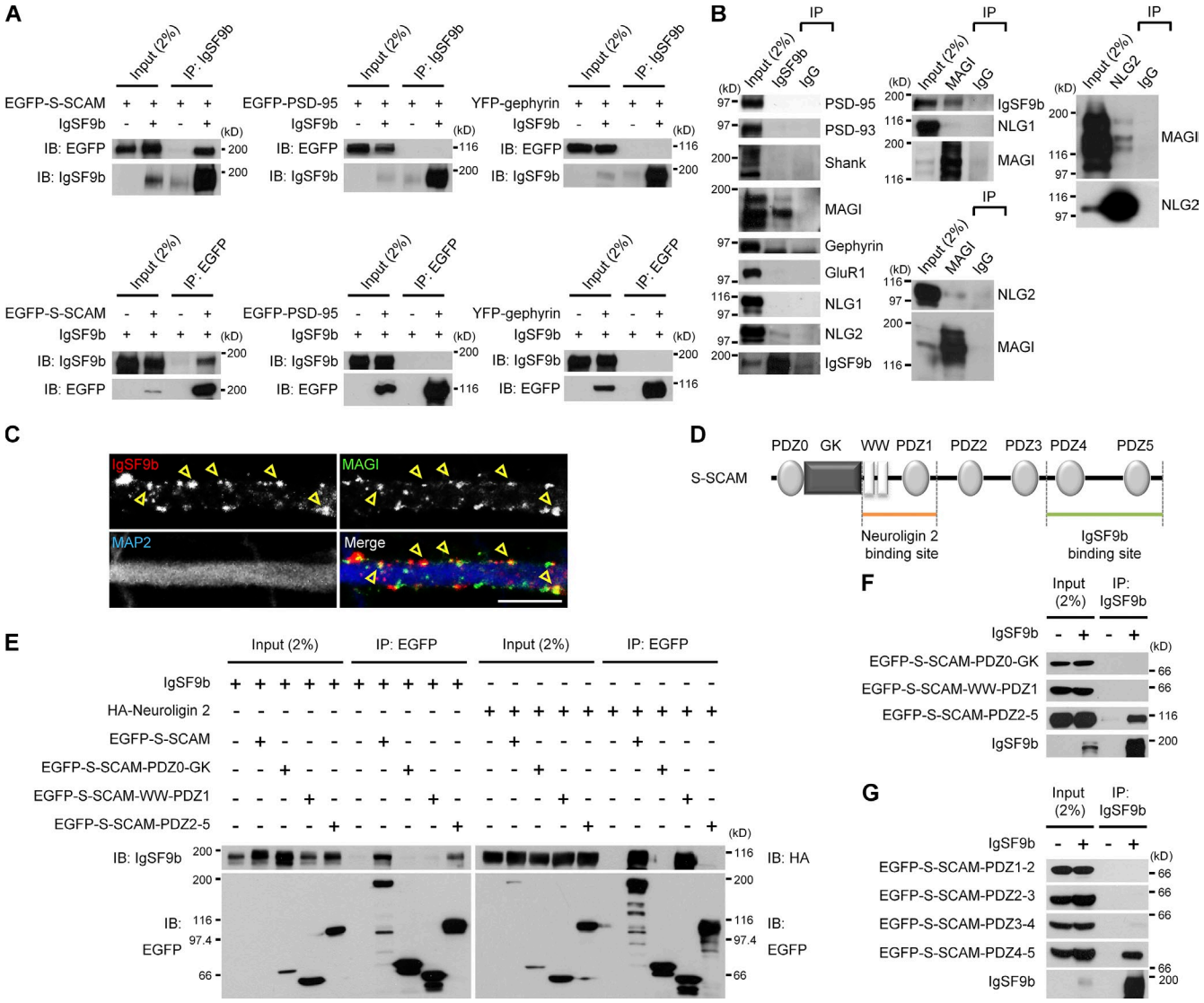

Figure 7. **IgSF9b interacts with S-SCAM at inhibitory synapses.** (A) IgSF9b forms a complex with S-SCAM, but not with PSD-95 or gephyrin, in heterologous cells. HEK293T cells transfected with IgSF9b (untagged) + tagged S-SCAM, PSD-95, or gephyrin were immunoprecipitated and immunoblotted with the indicated antibodies. The bottom panels indicate immunoprecipitation experiments performed in a reverse orientation. IP, immunoprecipitation; IB, immunoblot. (B) IgSF9b forms a complex with S-SCAM and neuroligin 2, but not with PSD-95, Shank, or neuroligin 1, in the brain. In addition, MAGI proteins form a complex with neuroligin 2. Lysates of the crude synaptosomal fraction from adult rat brains (6 wk) were immunoprecipitated with IgSF9b (left) or pan-MAGI (right) antibodies and immunoblotted. (C) IgSF9b colocalizes with MAGI proteins in cultured neurons. Cultured hippocampal neurons at DIV 16 were stained for endogenous IgSF9b, S-SCAM, and MAP2. Arrowheads indicate sites of colocalization. Bar, 10 µm. (D) Domain structure of S-SCAM. Neuroligin 2– or IgSF9b-binding regions are indicated. PDZ, PSD-95/Dlg/ZO-1 domain; GK, guanylate kinase-like domain. (E and F) PDZ2-5 of S-SCAM is sufficient for IgSF9b binding, whereas WW-PDZ1 mediates neuroligin 2 binding. EGFP–S-SCAM (full-length and deletion variants) cotransfected with IgSF9b or with HA-Neuroligin 2 in HEK293T cells were immunoprecipitated and immunoblotted. The absence of EGFP–S-SCAM band (~200 kD) in lane 2 is due to low expression levels of EGFP–S-SCAM and a limited film exposure. (G) PDZ4-5 domains of S-SCAM are sufficient for IgSF9b binding.

(MAGI-2), which is highly similar to MAGI-1 and known to be present at inhibitory synapses (Sumita et al., 2007). In an in vitro binding assay, IgSF9b formed a complex with S-SCAM but not with PSD-95 or gephyrin in HEK293T cells (Fig. 7 A). To assess endogenous association of IgSF9b with S-SCAM, we were limited by cross-reactivity of our anti–S-SCAM antibodies with MAGI-1 (Fig. S5, A and B), and thus assessed association of IgSF9b with S-SCAM using these pan-MAGI antibodies. In the brain, IgSF9b coprecipitated with MAGI proteins but not with other postsynaptic scaffolds including gephyrin, PSD-95, and Shank (Fig. 7 B). Notably, IgSF9b formed a weak complex with neuroligin 2 but not with neuroligin 1, which is consistent with its inhibitory synaptic localization. In addition, MAGI proteins formed a complex with neuroligin 2 (Fig. 7 B), which is consistent with the previously reported interaction between S-SCAM and neuroligin 2 (Sumita et al., 2007).

In cultured hippocampal neurons, IgSF9b colocalized with MAGI proteins on dendrites (Fig. 7 C). Furthermore, specifically in GABAergic interneurons, we found that MAGI proteins clustered at GAD67-positive inhibitory synapses, using both an antibody generated in this study (2015; Fig. S5, A and B), and an independent antibody (42574; Fig. S5, C and D). In addition, some MAGI proteins colocalized with vGlut1 clusters in interneurons (Fig. S5 E). To specifically test the localization

Published June 10, 2013

of S-SCAM independent of MAGI-1, we expressed tagged S-SCAM at a low level in cultured neurons. Exogenously expressed EGFP-tagged S-SCAM partially localized at VGAT-positive inhibitory synapses in both interneurons and pyramidal neurons (Fig. S5, F and G). This colocalization is in line with the previous finding that ~35% of S-SCAM clusters are detected at inhibitory synapses in cultured hippocampal neurons (Sumita et al., 2007). Collectively, these data suggest that S-SCAM is present at both excitatory and inhibitory synapses in interneurons, which is consistent with the molecular and biochemical associations

We next mapped minimal IgSF9b-binding domains in S-SCAM. Among the three deletion variants of S-SCAM tested (PDZ0–GK, WW–PDZ1, and PDZ2–5), PDZ2–5 was sufficient for IgSF9b binding (Fig. 7, D–F). WW–PDZ1 interacted with neuroligin 2, as previously reported (Sumita et al., 2007). Experiments with additional deletion variants of S-SCAM revealed that PDZ4–5 of S-SCAM is sufficient for IgSF9b binding (Fig. 7 G).

S-SCAM bridges IgSF9b and neuroligin 2

Because two distinct regions of S-SCAM bind IgSF9b and neuroligin 2 (Figs. 7 D and 8 A), we tested whether the three proteins can form a ternary complex. In heterologous cells, IgSF9b coprecipitated with neuroligin 2 only in the presence of S-SCAM (Fig. 8 B), which is consistent with the coprecipitation of IgSF9b with neuroligin 2 and MAGI proteins in the brain (Fig. 7 B). In addition, IgSF9b colocalized with both MAGI proteins and neuroligin 2, but not with PSD-95, in cultured interneurons (Fig. 8 C). These results suggest that IgSF9b forms a ternary complex with S-SCAM and neuroligin 2 at inhibitory synapses.

To see if S-SCAM is critically involved in linking IgSF9b and neuroligin 2 clusters in neurons, we tested whether S-SCAM knockdown decreases the colocalization between IgSF9b and neuroligin 2. We found that S-SCAM knockdown (sh-S-SCAM, DIV 15–20) in cultured interneurons suppressed the colocalization between IgSF9b and neuroligin 2, whereas it had no effect on the number of single IgSF9b or neuroligin 2 clusters (Fig. 8, D–G). A mutant knockdown construct that lacks the knockdown activity (sh-S-SCAM*) had no effect on the colocalization between IgSF9b and neuroligin 2. In addition, S-SCAM knockdown decreased the number of VGAT-positive gephyrin clusters (Fig. 8, H and I). These results suggest that S-SCAM is required for the close association between IgSF9b- and neuroligin 2–containing subsynaptic domains in interneurons, and that S-SCAM is required for the development or maintenance of inhibitory synaptic structures containing gephyrin and VGAT.

IgSF9b and neuroligin 2 bidirectionally drive protein clustering

The formation of the ternary complex between IgSF9b, S-SCAM, and neuroligin 2 may be driven unidirectionally by IgSF9b or neuroligin 2, or bidirectionally. To test this idea, HEK293T cells triply expressing IgSF9b, S-SCAM, and neuroligin 2 were incubated with preclustered neurexin β1 ectodomain to induce neuroligin 2 aggregation. This aggregation induced coclustering of IgSF9b only in the presence of S-SCAM in heterologous cells (Fig. 9 A). In cultured hippocampal neurons treated with preclustered neurexin β1, primary clustering of endogenous neuroligin 2 induced coclustering of MAGI proteins and IgSF9b at subcellular sites lacking VGAT (Fig. 9, B and C).

Conversely, in cultured neurons expressing N-terminally EGFP-tagged IgSF9b, direct aggregation of IgSF9b by GFP antibody–coated beads induced coclustering of endogenous neuroligin 2 at sites that lack synapsin I (Fig. 9, D and E). These results suggest that the formation of the ternary complex containing IgSF9b, S-SCAM, and neuroligin 2 can be driven bidirectionally, initiating from neuroligin 2 or IgSF9b.

Neuroligin 2 does not affect the general stability or synaptic localization of IgSF9b

IgSF9b and neuroligin 2, which can bidirectionally drive protein clustering, may also regulate the synaptic localization or general stability of each other. However, neuroligin 2 deletion in mice, which has been reported previously (Varoqueaux et al., 2006), had no effect on overall levels of IgSF9b, as determined by immunoblot analysis of whole-brain lysates (Fig. 9, F and G). In addition, neuroligin 2 deficiency had no effect on synaptic levels of IgSF9b, as determined by immunoblot analysis of synaptic brain fractions including synaptosomal membranes and PSD fractions where IgSF9b is highly enriched (Fig. 9, F and G). These results suggest that neuroligin 2 has minimal influences on overall stability or synaptic localization of IgSF9b.

Gephyrin can be clustered by neuroligin 2 but not by IgSF9b

Because IgSF9b can drive coclustering of neuroligin 2 (Fig. 9, D and E), we tested whether IgSF9b can also drive coclustering of gephyrin, an inhibitory postsynaptic scaffold that directly interacts with neuroligin 2 (Poulopoulos et al., 2009) and diverse inhibitory postsynaptic proteins including $GABA_A$ and glycine receptors and signaling, cytoskeletal, and trafficking proteins (Fritschy et al., 2008). However, bead aggregation of IgSF9b in cultured neurons did not induce coclustering of gephyrin (Fig. 10, A and B), despite the fact that it could cocluster neuroligin 2 (Fig. 10 C). In contrast, bead aggregation of neuroligin 2 could induce coclustering of gephyrin at VGAT-negative sites, whereas CD4 (a negative control) could not (Fig. 10, A and B). Similarly, neuroligin 2 aggregation by preclustered neurexin β1 induced gephyrin coclustering (Fig. 9 B). These results suggest that gephyrin can be clustered by neuroligin 2 but not by IgSF9b.

Discussion

IgSF9b, a novel inhibitory synaptic adhesion molecule

In the present study, we have identified IgSF9b as a novel inhibitory synaptic adhesion molecule.

IgSF9b differs from Dasm1/IgSF9 in several aspects. Dasm1 is mainly localized at and regulates excitatory synapses (Shi et al., 2004a,b), whereas IgSF9b mainly regulates inhibitory synapses. In addition, Dasm1 does not associate with IgSF9b (Fig. 3 A), despite the fact that they show substantial amino acid identity in

Published June 10, 2013

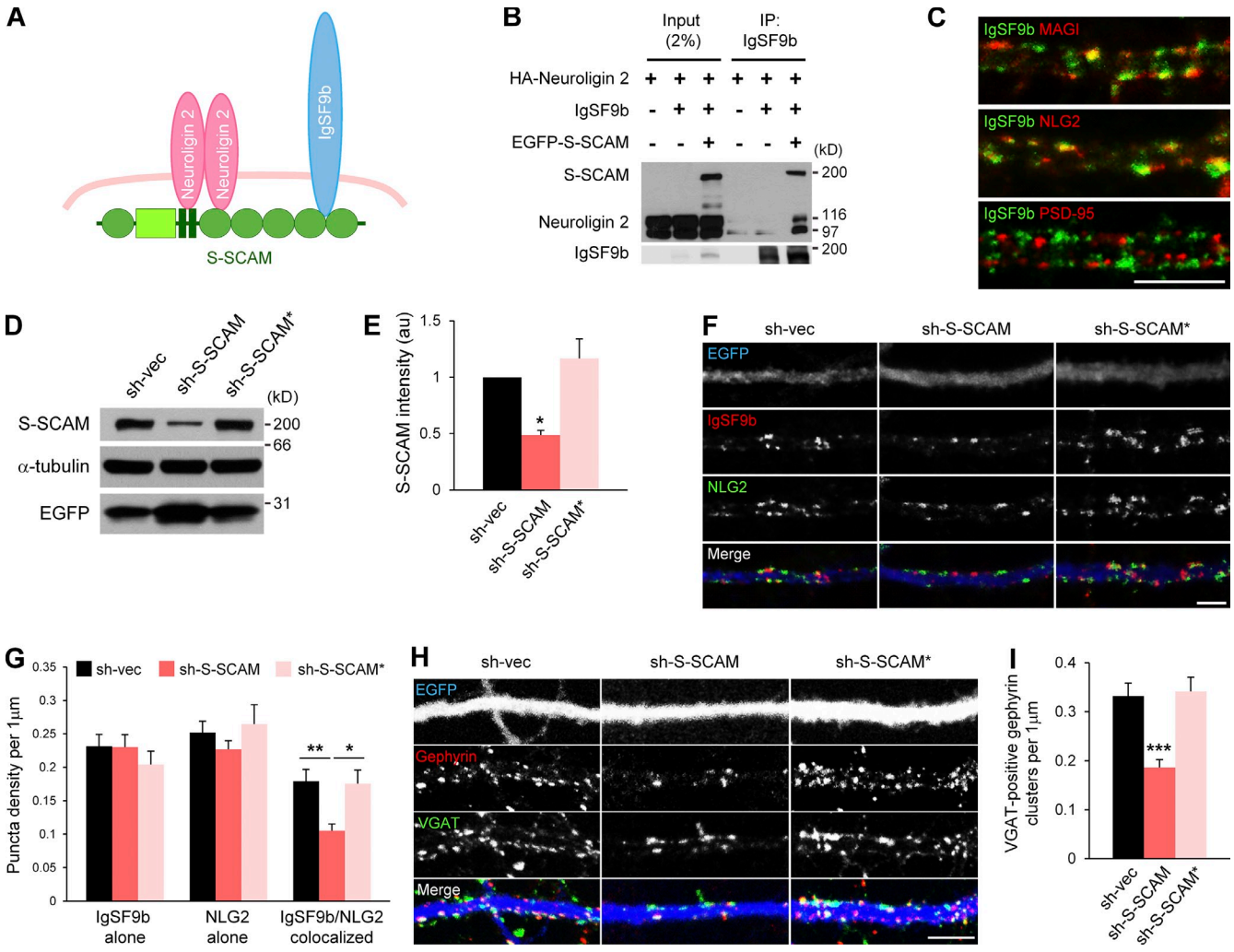

Figure 8. **S-SCAM bridges IgSF9b and neuroligin 2.** (A) A schematic diagram showing that IgSF9b and neuroligin 2 bind to two distinct regions of S-SCAM (PDZ4-5 and WW-PDZ1, respectively), forming a ternary complex. (B) IgSF9b forms a ternary complex with S-SCAM and neuroligin 2 in HEK293T cells, as determined by coimmunoprecipitation analysis. (C) IgSF9b colocalizes with MAGI and neuroligin 2 proteins, but not with PSD-95, in cultured hippocampal interneurons (DIV 18–23). NLG2, neuroligin 2. (D) A S-SCAM knockdown construct (sh-S-SCAM), but not a mutant sh-S-SCAM that lacks knockdown activity (sh-S-SCAM*), reduces expression of S-SCAM in HEK293T cells. HEK293T cells were doubly transfected with EGFP–S-SCAM + sh-S-SCAM, sh-vec (empty shRNA vector), or sh-S-SCAM*, and immunoblotted with the indicated antibodies. EGFP (size corresponds to plain EGFP coexpressed from the sh-vectors not the EGFP–S-SCAM fusion) and α-tubulin were visualized for normalization. (E) Quantification of the results from D. Integrated band intensities of S-SCAM were normalized to that in the control lane (sh-vec). $n = 3$; *, $P < 0.05$; ANOVA and Tukey's multiple comparison test. (F and G) Knockdown of S-SCAM reduces colocalization between IgSF9b and neuroligin 2. Cultured hippocampal neurons were transfected with sh-S-SCAM, sh-vec, or sh-S-SCAM* (DIV 15–20), and immunostained for the indicated proteins, and interneurons were selected for colocalization analysis. $n = 19$ for sh-vec, 19 for sh-S-SCAM, and 11 for sh-S-SCAM*. *, $P < 0.05$; **, $P < 0.01$; ANOVA and Tukey's multiple comparison test were used. (H and I) S-SCAM knockdown reduces the number of VGAT-positive gephyrin clusters in interneurons. Cultured hippocampal neurons were transfected with sh-S-SCAM, sh-vec, or sh-S-SCAM* (DIV 15–20), and immunostained for the indicated proteins. $n = 18$ for sh-vec, 17 for sh-S-SCAM, and 12 for sh-S-SCAM*. ***, $P < 0.001$; ANOVA and Tukey's multiple comparison test. Error bars indicate mean ± SEM. Bars: (C) 10 µm; (F) 5 µm; (H) 10 µm.

their extracellular domains (Fig. S1 A). Given that their cytoplasmic domains are quite dissimilar in amino acid sequences, we predict that IgSF9b and Dasm1 have distinct intracellular partners mediating different intracellular signaling pathways.

IgSF9b, to the best of our knowledge, represents the fourth adhesion molecule that is selectively present at inhibitory synapses, next to neuroligin 2, dystroglycan, and slitrk3 (Lévi et al., 2002; Varoqueaux et al., 2004; Takahashi et al., 2012).

Of these four proteins, IgSF9b may stand out as a unique protein for the following reasons. First, it localizes and functions at a distinct subset of inhibitory synapses, which is consistent with the known heterogeneity of inhibitory synapses (Lévi et al., 2002; Varoqueaux et al., 2004; Fritschy et al., 2012). In culture, IgSF9b contributes mainly to inhibitory synapses onto GABAergic interneurons, onto the majority if not all GABAergic neurons (Fig. 1), and is thus not selective for interneuron type. Expression patterns in vivo also suggest selective function of IgSF9b in interneurons, although some levels of expression are also observed in cortical and hippocampal CA1 pyramidal cells and cerebellar granule cells. Our study did not explore how IgSF9b contributes to interneuronal circuitry in the brain. However, in dissociated hippocampal cultures, knockdown of postsynaptic IgSF9b in GABAergic interneurons suppresses inhibitory synapse number and synaptic transmission onto these neurons, whereas the same

Published June 10, 2013

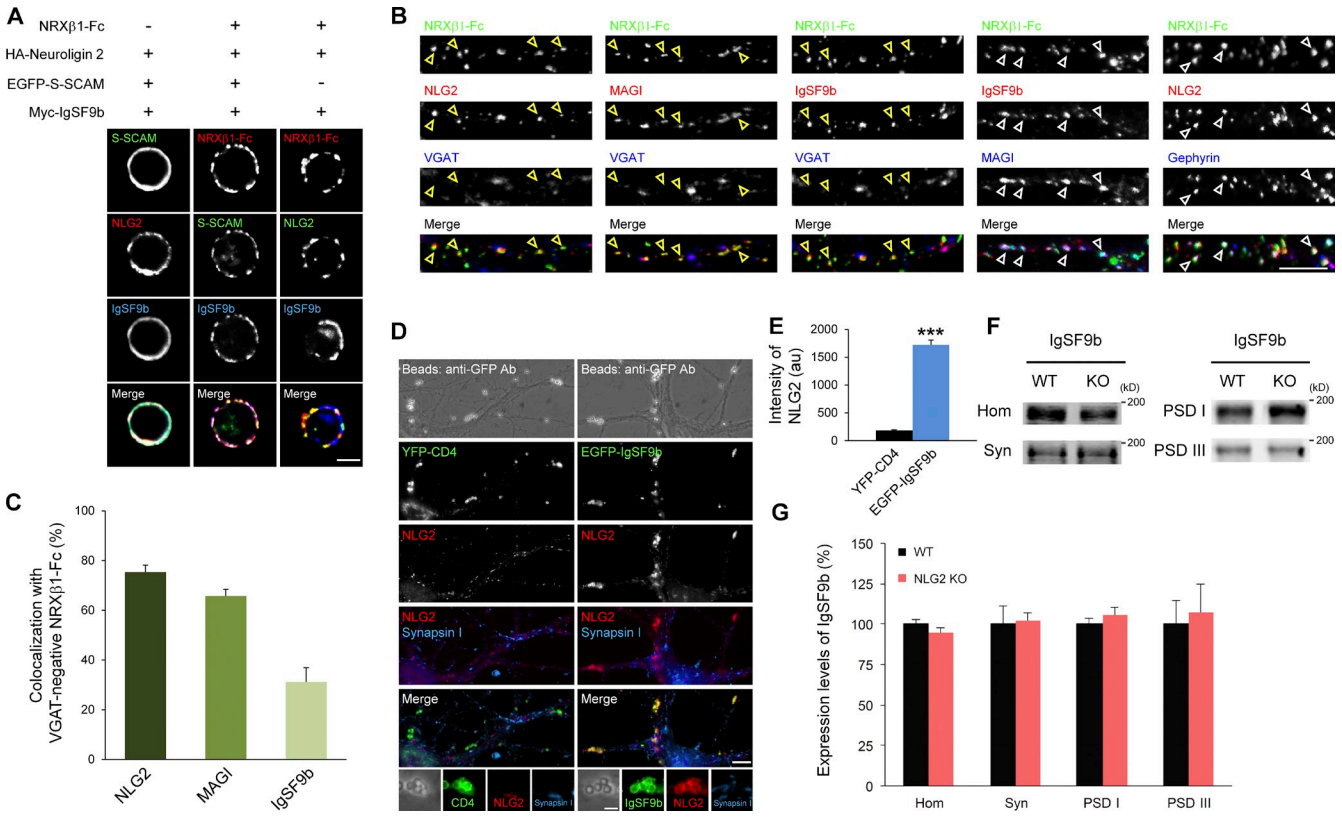

Figure 9. **IgSF9b and neuroligin 2 bidirectionally drive protein clustering.** (A) Aggregation of neuroligin 2 by preclustered neurexin β1-Ecto-Fc (NRXβ1-Fc) induces coclustering of IgSF9b only in the presence of S-SCAM in heterologous cells. HEK293T cells expressing combinations of HA-Neuroligin 2 (NLG2), EGFP–S-SCAM, and Myc-IgSF9b were incubated with preclustered NRXβ1-Fc and stained for HA, Myc, EGFP, or Fc. Not all proteins could be visualized for the shortage of staining channels. (B and C) Neuroligin 2 aggregation by preclustered NRXβ1-Fc induces coclustering of endogenous MAGI, IgSF9b, and gephyrin at VGAT-negative subcellular sites in neurons. Cultured hippocampal neurons were incubated with NRXβ1-Fc (DIV 16–17) and immunostained for the indicated proteins. The arrowheads indicate sites of NRXβ1-Fc clustering. The quantifications represent percent colocalization of the indicated proteins (neuroligin 2, MAGI, and IgSF9b) with NRXβ1-Fc clusters. (D) Direct bead aggregation of IgSF9b induces neuroligin 2 coclustering at synapsin I–negative sites in neurons. Cultured hippocampal neurons expressing N-terminally EGFP-tagged IgSF9b, or YFP-tagged CD4 (control; DIV 9–14), were incubated with GFP antibody-coated beads for 24 h and visualized at DIV 15 by double immunofluorescence staining for neuroligin 2 (NLG2) and synapsin I. (E) Quantification of the results from D, as measured by mean intensities of neuroligin 2 around beads. $n = 81$ beads from 24 cells for EGFP-IgSF9b, and $n = 181$ beads from 30 cells for YFP-CD4. ***, $P < 0.001$; Student's t test. (F and G) Deletion of neuroligin 2 in mice has minimal effects on overall stability or synaptic localization of IgSF9b. Whole brain homogenates (Hom) and synaptic fractions such as synaptosomal membranes (Syn) and PSD fractions (PSD I and PSD III) from adult mice brain (4–8 wk) were immunoblotted for IgSF9b. (G) Quantification of the results from F. IgSF9b levels were normalized to total protein loading, and then to the mean sample value of all lanes on the same blot to correct for blot-to-blot variance. $n = 6$ mice for both wild-type (WT) and neuroligin 2 knockout (KO). Error bars indicate mean ± SEM. Bars: (A and B) 10 µm; (D, top panels) 10 µm; (D, insets) 2 µm.

knockdown in pyramidal neurons has no effect (Fig. 4 and Fig. S4). If IgSF9b has a similar function in vivo, it could be an interesting general regulator of inhibitory transmission selectively among GABAergic neurons. Although dystroglycan also localizes to a subset of GABAergic synapses (Lévi et al., 2002) and neuroligin 2 may contribute functionally to specific subsets of GABAergic synapses (Gibson et al., 2009; Poulopoulos et al., 2009), this selectivity of IgSF9b for GABAergic synapses onto GABAergic neurons appears unique.

Second, IgSF9b is distinct in that it is a homophilic cell adhesion molecule (Fig. 3), whereas neuroligin 2, dystroglycan, and slitrk3 are not. Based on this feature, it is likely that the synaptic IgSF9b observed here represents both presynaptic and postsynaptic pools. Given that postsynaptic knockdown of IgSF9b reduces inhibitory synapse number and function in GABAergic interneurons, postsynaptic IgSF9b appears to be important. We suspect that IgSF9b may act from the presynaptic side as well, through trans-synaptic homophilic adhesion, although additional experiments will be required to explore this possibility.

Third, IgSF9b is not sufficient to trigger synapse formation (Fig. 3), whereas neuroligin 2 and slitrk3 have such activities. The developmental expression of IgSF9b also lags behind that of neuroligin 2 (Fig. 2), and IgSF9b appears at inhibitory synapses in hippocampal cultures at a late stage of their development (Fig. S2). Therefore, IgSF9b may stabilize the inhibitory synapses initially organized by other adhesion molecules.

Lastly, IgSF9b can be coclustered by presynaptic neurexin via neuroligin 2, whereas dystroglycan is not (Graf et al., 2004), which suggests that IgSF9b is an inhibitory adhesion molecule closely associated with the neurexin–neuroligin system.

Subsynaptic domains at inhibitory synapses

Our super-resolution data indicate that IgSF9b and gephyrin/$GABA_A$ receptors (γ2) distribute to two distinct inhibitory

Published June 10, 2013

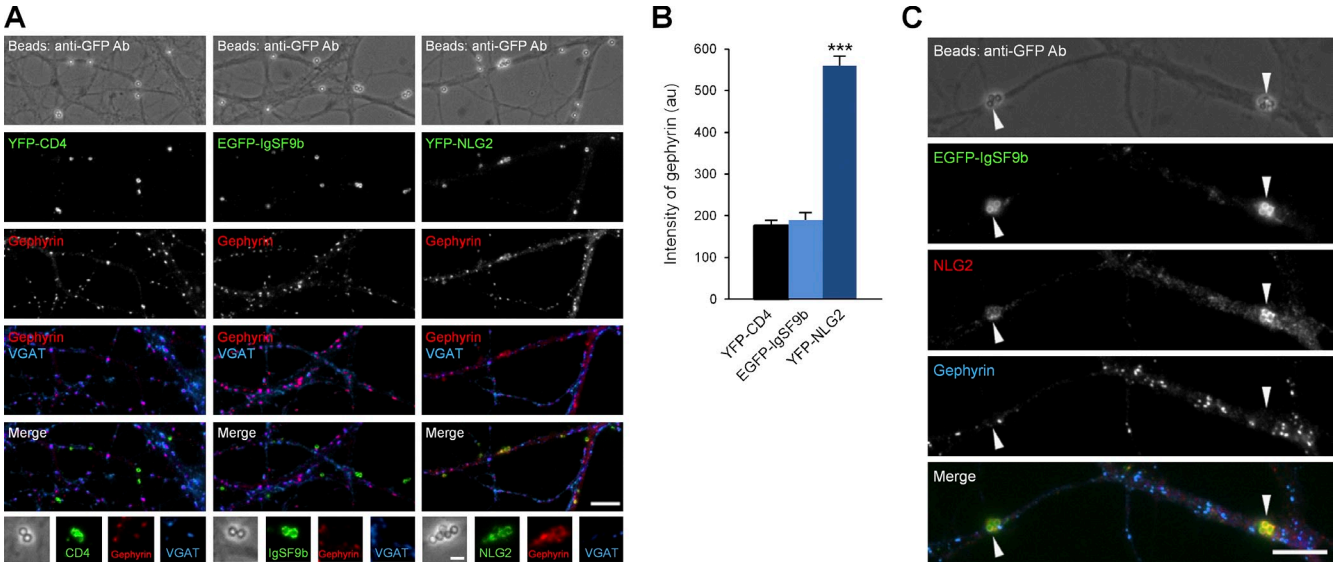

Figure 10. **Gephyrin can be clustered by neuroligin 2 but not by IgSF9b.** (A) Cultured hippocampal neurons expressing N-terminally EGFP/YFP-tagged IgSF9b (EGFP-IgSF9b), neuroligin 2 (YFP-NLG2), or CD4 (YFP-CD4; negative control; DIV 19–21), were incubated with GFP antibody–coated beads for 24 h and visualized at DIV 22 by double immunofluorescence staining for gephyrin and VGAT. Bars: (top) 10 µm; (insets) 2 µm. (B) Quantification of the results from A, as measured by mean intensities of gephyrin around beads. Error bars indicate mean ± SEM. n = 150, 104, 109 beads from 22, 21, and 21 neurons for YFP-CD4, EGFP-IgSF9b, and YFP-NLG2, respectively. ***, $P < 0.001$; ANOVA and Tukey's multiple comparison test compared with YFP-CD4. (C) Cultured hippocampal neurons expressing EGFP-IgSF9b clustered with GFP antibody–coated beads as above (in A) were immunolabeled for neuroligin 2 and gephyrin. Bar, 10 µm.

subsynaptic domains (Fig. 6). This suggests that the two subsynaptic domains may have distinct functions. What would be the functions?

One possibility is that the IgSF9b-containing domain may mediate synaptic adhesion, given that IgSF9b can mediate homophilic adhesion, which may act synergistically with the adhesion mediated by neurexin and neuroligin 2. Meanwhile, the $GABA_A$ receptors/gephyrin-containing domain may mediate inhibitory synaptic transmission by responding to presynaptic GABA. The two subsynaptic domains must be linked functionally, together mediating GABAergic synapse development and maintenance, as knockdown of IgSF9b in interneurons reduces VGAT-positive gephyrin clusters and reduces mIPSC frequency.

Distinct subsynaptic localization of receptors and adhesion molecules have been reported for excitatory synapses, where NMDA and AMPA glutamate receptors are present in the central region of the synapse (Baude et al., 1993; Chen et al., 2008), whereas metabotropic glutamate receptors and homophilic adhesion molecules such as *N*-cadherin are localized in the periphery of the synapse (Uchida et al., 1996). However, a unique feature of our current finding is that the two subsynaptic domains do not display a concentric circular arrangement as in excitatory synapses. Rather, the two subsynaptic domains have diverse sizes and shapes, and randomly contact with each other, forming diverse overall shapes.

Why are there two distinct subsynaptic domains, rather than all the synaptic proteins being randomly mixed throughout the synapse? It is conceivable that the two functionally distinct subsynaptic domains, one for adhesion and the other for transmission, could easily be joined or separated for rapid and efficient formation and elimination of functional synapses. Each subsynaptic domain may even represent a preassembled packet, as previously suggested for predetermined postsynaptic hotspots for development of functional excitatory synapses (Gerrow et al., 2006) and for rapid and efficient assembly of presynaptic active zones (Zhai et al., 2001; Shapira et al., 2003).

S-SCAM as an adaptor bridging IgSF9b and neuroligin 2

Our data suggest that S-SCAM is important for physical coupling of the two inhibitory subsynaptic domains. In support of this notion, S-SCAM forms a ternary complex with IgSF9b and neuroligin 2 (Fig. 8). Moreover, S-SCAM knockdown enhances mislocalization of IgSF9b and neuroligin 2 (Fig. 8). What would be the advantages of S-SCAM as a bridging molecule?

S-SCAM is a protein with multiple domains for protein–protein interactions (i.e., six PDZ domains) and many known binding partners. Therefore, S-SCAM may be able to function as a focal site of multiprotein interaction and assembly that would support a dynamic and regulated association between the two subsynaptic domains. Known S-SCAM–binding proteins thus far include neuroligin 1, neuroligin 2, NMDA receptors, GKAP/SAPAP, and SynArfGEF (Hirao et al., 1998; Kim and Sheng, 2004; Fukaya et al., 2011), where only neuroligin 2 and SynArfGEF are inhibitory synaptic proteins. SynArfGEF, a guanine nucleotide exchange factor for the Arf6 small GTPases, is preferentially localized at inhibitory synapses, and directly interacts with dystrophin/utrophin (Fukaya et al., 2011), which, together with dystroglycan, are components of the dystrophin-associated glycoprotein complex. Therefore, S-SCAM has the potential to regulate Arf-dependent synaptic membrane/protein trafficking at the junction between the two subsynaptic domains, and to position the dystrophin-associated glycoprotein complex close to this junction.

Published June 10, 2013

This concept of a multidomain connector for neighboring macromolecular structures is reminiscent of the finding that dynamin-3, a GTPase with multiple domains for protein–protein interactions, positions the endocytic zone, an excitatory postsynaptic hotspot for local AMPA receptor endocytosis (Blanpied et al., 2002), close to the PSD via its direct interaction with Homer, a PDZ and EVH1 domain–containing adaptor protein in the PSD (Lu et al., 2007).

Bidirectional protein clustering by IgSF9b and neuroligin 2

As in excitatory synapses, molecular organization of inhibitory postsynaptic protein complexes involves key synaptic scaffolding proteins such as gephyrin (Fritschy et al., 2008, 2012; Tyagarajan and Fritschy, 2010; Sheng and Kim, 2011). Gephyrin forms homomultimers and interacts with diverse postsynaptic membrane, signaling, and cytoskeletal proteins. This gephyrin-based postsynaptic protein assembly is thought to be initiated by the clustering of neuroligin 2 driven by presynaptic neurexins (Craig and Kang, 2007; Südhof, 2008; Shen and Scheiffele, 2010; Krueger et al., 2012). Our results extend this view of inhibitory postsynaptic assembly. Specifically, initial clustering of neuroligin 2 appears to induce coclustering of S-SCAM and IgSF9b, in addition to gephyrin, in order to strengthen synaptic adhesion.

Therefore, functions of neuroligin 2 as a postsynaptic organizer at inhibitory synapses appear to be multifold. They are to induce clustering of (1) gephyrin and associated proteins for postsynaptic differentiation, (2) S-SCAM and IgSF9b for lateral association with a subsynaptic adhesive domain, and (3) presynaptic neurexins for presynaptic differentiation.

Our data suggest that IgSF9b and neuroligin 2 can reciprocally cluster each other (Fig. 9). Possible functions of neuroligin 2 clustering by IgSF9b are unclear. Postsynaptic assembly in this direction may have a limited impact given the findings from the artificial aggregation assays that IgSF9b drives protein clustering up to neuroligin 2 but not beyond to gephyrin, whereas neuroligin 2 can cluster gephyrin in addition to IgSF9b. However, the bidirectional clustering between IgSF9b and neuroligin 2 may enhance the chance or rate of forming the connection between the two subsynaptic domains. Altogether, the reciprocal clustering of IgSF9b and neuroligin 2 is likely to enhance the development and stabilization of inhibitory synapses, particularly in interneurons where IgSF9b is abundant.

In conclusion, our data identifies a novel inhibitory synaptic adhesion molecule IgSF9b that localizes to a distinct subsynaptic domain and is coupled to neuroligin 2 via S-SCAM to promote inhibitory synaptic development. A direction for future studies would be to explore the functional significance of the two subsynaptic domains, and related regulatory mechanisms. The selective localization and function of IgSF9b at inhibitory synapses onto GABAergic interneurons, at least in culture, place IgSF9b in a unique position among inhibitory synaptic adhesion proteins and identify it as a potential drug target. Paradoxically, we predict that down-regulation of IgSF9b level or function, through selectively reducing inhibition onto GABAergic neurons, may increase GABAergic transmission to pyramidal cells and reduce overall circuit excitation

Materials and methods

DNA constructs

Full-length mouse IgSF9b (accession no. NM_001129787, original GenBank version, aa 1–1,441) was amplified by PCR from a mouse brain cDNA library (BD) and subcloned into pEGFP-N1 (Takara Bio Inc.) with an intact stop codon at the 3′ end. Untagged IgSF9b was generated by subcloning of full-length IgSF9b (aa 1–1,441) into pGW1 (British Biotech). Myc epitope (EQKLISEEDL) and EGFP was inserted between residues 28 and 29 of IgSF9b in pGW1 and pEGFP-N1, respectively. Ecto-domains of IgSF9b (aa 1–716) were subcloned into pEGFP-N1 in which EGFP was replaced with human Fc and pDisplay (Invitrogen). The C-terminally Flag-tagged IgSF9b that lacks a cytosolic region (aa 1–756) was subcloned into pEGFP-N1, which has triple Flag motifs with a stop codon. For the yeast two-hybrid assay, the last 75 aa of IgSF9b were subcloned into pBHA (bait vector). For siRNA knockdown, nucleotides 216–234 (5′-CATCAAGTTTGGCTACTAT-3′) of rat IgSF9b, its point mutant (5′-CATAAAGTTCGGCTACTAT-3′), nucleotides 1,328–1,346 (5′-GAGATGAGCCGGACGAGTT-3′) of rat S-SCAM, and its point mutant (5′-GAGACGAGCCTGATGAGTT-3′) were selected and subcloned into pSuper.gfp/neo (OligoEngine). For N-terminally EGFP tagged S-SCAM, full-length rat S-SCAM (GenBank accession no. NM_053621, aa 1–1,277) was amplified from untagged S-SCAM and subcloned into pEGFP-C1 (Takara Bio Inc.). The following deletion variants of S-SCAM were also subcloned into pEGFP-C1: PDZ0-GK (aa 1–301), WW-PDZ1 (aa 296–578), PDZ2-5 (aa 573–1,277), PDZ1-2 (aa 417–710), PDZ2-3 (aa 573–892), PDZ3-4 (aa 747–1,028), and PDZ4-5 (aa 867–1,277). For N-terminally EGFP-tagged MAGI-1, full-length rat MAGI-1 (NM_001030045, aa 1–1,255) was amplified from a rat brain cDNA library (BD) and subcloned into pEGFP-C1. The following expression constructs have been described previously: YFP-gephyrin (rat gephyrin isoform 2.6 was subcloned into modified pLentiLox3.7; Dobie and Craig, 2011), HA-NLG2 (a gift from P. Scheiffele, Biozentrum of the University of Basel, Basel, Switzerland; mouse neuroligin-2 was subcloned into pNICE; Scheiffele et al., 2000), YFP-CD4 (a mature form of CD4 was subcloned into spYFP-C1; Takahashi et al., 2011), YFP-NLG2 (modified from HA-NLG2; Graf et al., 2004), untagged S-SCAM (from Y. Hata, Graduate School of Medicine, Tokyo Medical and Dental University, Tokyo, Japan; full-length rat S-SCAM was subcloned into pCMV5; Hirao et al., 1998), and NRXβ1-Fc (pCMVIgbN1β-1 from T.C. Sudhof, Stanford University Medical School, Stanford, CA; aa 1–300 of rat neurexin-1β lacking an insert in splice site #4 was subcloned into pCMV-Ig; Ko et al., 2009).

Antibodies

Guinea pig (1593) and rabbit (1913) polyclonal IgSF9b antibodies were raised against GST-IgSF9b aa 1,126–1,351 (226 aa) and aa 1,293–1,441 (149 aa), respectively. GST–S-SCAM aa 303–405 (103 aa, WW domains) was used as an immunogen to generate guinea pig (2015) and rabbit (2013) polyclonal S-SCAM antibodies. The following antibodies have been described previously: EGFP (1432, guinea pig, H6-EGFP aa 1–240; Choi et al., 2006), PSD-95 (SM55, rabbit, H6-PSD-95 aa 77–299; Choi et al., 2002), neuroligin 2 (rabbit, RGGGVGADPAEALRPACP; Varoqueaux et al., 2004; Graf et al., 2006), S-SCAM (1146, rabbit, H6-S-SCAM aa 341–711; Mok et al., 2002), S-SCAM (42574, rabbit, GST–S-SCAM aa 303–405, a gift from Y. Hata), PSD-93 (1634, rabbit, GST–PSD-93, full-length; Kim et al., 2009), Shank (1123, guinea pig, GST-Shank1 aa 469–691; Lim et al., 2001), and GluR1 (1193, rabbit, SHSSGM-PLGATGL; Kim et al., 2009). The following antibodies are commercially available: $GABA_AR\gamma2$, vGlut1, VGAT, gephyrin, neuroligin 2 (Synaptic Systems); neuroligin1, Myc, and HA (Santa Cruz Biotechnology, Inc.); IgSF9b (HPA010802; rabbit), MAP2, α-tubulin, Flag, and synaptophysin (Sigma-Aldrich); PSD-95 (Thermo Fisher Scientific); $GABA_AR\alpha1$ (Alomone Labs); GAD67, synapsin I (EMD Millipore), and GAD65 (Developmental Studies Hybridoma Bank); GAD65/67 (Enzo Life Sciences); and Cy3-conjugated anti-Fc (Jackson ImmunoResearch Laboratories, Inc.).

Deglycosylation assay

Enzymatic deglycosylation was performed with rat P2 (crude synaptosomes) fractions extracted with 1% deoxycholate (DOC) using *N*-glycosidase/PNGase F (New England Biolabs, Inc.), sialidase/neuraminidase (Roche), and *O*-glycosidase/endo-α-*N*-acetylgalactosaminidase (EMD Millipore) according to the manufacturer's instructions.

In situ hybridization analysis

In situ hybridization was performed as described previously (Kim et al., 2003). In brief, adult rats and mice brains (6 wk) were rapidly extracted

Published June 10, 2013

and frozen in isopentane. Brain sections (12 µm thick) were prepared with a cryostat (CM 3000; Leica) and then thaw-mounted on gelatin-coated glass slides. Sections were fixed in 4% paraformaldehyde, washed with PBS, acetylated with 0.25% acetic anhydrides in 0.1 M triethanolamine/0.9% NaCl, pH 8.0, dehydrated in ethanol and chloroform, and then air-dried. A rat IgSF9b antisense riboprobe corresponding to nt 3,532–4,164 (633 bp) was generated by RNA polymerase transcription using a Riboprobe System (Promega) in the presence of α-[^{35}S]-UTP. The sections were hybridized with ^{35}S-labeled probes at 52°C overnight, and then washed four times in 4× SSC solution at room temperature. Subsequently, the slides were incubated with RNase buffer at 37°C for 30 min and washed. Slides were dehydrated, air-dried, exposed, and developed in a developer (D-19; Kodak). For in situ hybridization using mouse brain sections, we used the following mouse IgSF9b antisense riboprobes: nt 325–960 (636 bp) for probe "a," nt 3,428–3,999 (572 bp) for probe "b" (with the last 4 nt corresponding to mRNA of IgSF9b-2), and nt 3,995–4,326 (332 bp) for probe "c."

Brain fractionation and coimmunoprecipitation

Subcellular and PSD fractions of adult rat and mouse brains were prepared as described previously (Carlin et al., 1980; Huttner et al., 1983). In brief, rat brain homogenates (H) were centrifuged at 1,000 *g* to remove nuclei and other large debris (P1). The supernatant was centrifuged at 10,000 *g* to obtain a crude synaptosome fraction (P2), and the supernatant (S2) was further centrifuged at 160,000 *g* to obtain light membranes (P3) and cytosol fractions (S3). In parallel, the P2 fraction was subjected to hypotonic lysis and centrifuged at 25,000 *g* to precipitate synaptosomal membranes (LP1). The supernatant (LS1) was further centrifuged at 160,000 *g* to obtain a crude synaptic vesicle-enriched fraction (LP2) and soluble fraction (LS2). To obtain PSD fractions, the synaptosomal fraction was extracted with detergents, once with Triton X-100 (PSD I), twice with Triton X-100 (PSD II), and once with Triton X-100 and once with Sarkosyl (PSD III). Protein loading was quantified using the Pierce Reversible Protein Stain kit (Thermo Fisher Scientific). For in vivo coimmunoprecipitation, the P2 fraction of adult rat brain was extracted in buffer containing 1% sodium deoxycholate and 50 mM Tris-HCl, pH 9.0, followed by incubation with immunoprecipitation antibodies. For coimmunoprecipitation in heterologous cells, cells were extracted in phosphate buffered saline containing 1% Triton X-100.

Coculture assay

Coculture assays were performed as described previously (Kim et al., 2006; Biederer and Scheiffele, 2007). In brief, primary hippocampal neuron cultures at DIV 10 prepared from embryonic day 18–19 rats were cocultured with HEK293T cells expressing pDisplay-IgSF9b or EGFP. The cocultured cells were immunostained with synapsin1, PSD-95, or gephyrin antibodies.

Neuron culture, transfection, and immunocytochemistry

Primary hippocampal neuronal cultures were prepared from embryonic day 18–19 rat hippocampi as described previously (Goslin and Banker, 1991). Cultures were plated on coverslips coated with poly-L-lysine and laminin, and grown in neurobasal medium supplemented with B27 (Invitrogen) and 2% fetal bovine serum (Gibco) in a 10% CO_2 incubator. Cultured neurons were transfected using a calcium phosphate transfection kit (Takara Bio Inc. and Promega) and fixed with 4% paraformaldehyde/4% sucrose, permeabilized with 0.2% Triton X-100 in PBS, and incubated with the specific primary antibodies. Secondary antibodies were conjugated with Cy3, Cy5, or FITC (Jackson ImmunoResearch Laboratories, Inc.) or with Alexa Fluor 488, Alexa Fluor 568, or Alexa Fluor 647 (Invitrogen). For the application of preclustered neurexin1β ectodomain (NRXβ1-Fc) to cultured neurons, preclustered NRXβ1-Fc was generated by preincubation of Cy3-conjugated anti-Fc antibody with NRXβ1-Fc in neuronal culture medium and incubated with hippocampal cultures for 24 h (DIV 16–17). For the bead clustering assay, nonfluorescent Neutravidin FluoSpheres (F-8777; Invitrogen) were rinsed in PBS containing 100 µg/ml BSA (PBS/BSA) and incubated with biotin-conjugated anti-GFP (which can also recognize YFP; Rockland Immunochemicals) at ∼6 µg antibody/µl beads in PBS/BSA at RT for 2 h. Beads were applied to hippocampal neuron cultures for 24 h.

Image acquisition and quantification

Fluorescent images were randomly acquired as z stacks using a confocal microscope (LSM510; Carl Zeiss) or on an epifluorescence microscope (Axioplan; Carl Zeiss) using C-Apochromat 63×, 1.20 NA water-immersion or 63×, 1.40 NA oil-immersion objective lenses at room temperature and analyzed with MetaMorph image analysis software (Universal Imaging). Inhibitory interneurons were distinguished from excitatory pyramidal neurons by immunostaining with GABAergic neuronal markers such as GAD67 and/or by morphological aspects such as polygonal shaped cell bodies, less spiny and nontapered dendrites with longer segments between branch points (Benson et al., 1994). To determine the density of synaptic protein clusters, every primary dendritic segment encompassing 50 µm from cell bodies of each neuron was analyzed. For quantitation of images from coculture assays, all captured images were thresholded and the integrated intensity of the clusters on transfected HEK293T cells was normalized to the cell area. All values are presented as mean ± SEM and analyzed by Student's *t* test or one-way analysis of variance (ANOVA) with Tukey's multiple comparison test.

For STORM analysis, neurons were rinsed and fixed with 3% formaldehyde and 0.1% glutaraldehyde, and primary antibodies (2.5 µg/ml anti-gephyrin, 2 µg/ml rabbit anti-IgSF9b, and 2.5 µg/ml guinea pig anti–$GABA_AR$ γ2). Secondary antibodies (Jackson ImmunoResearch Laboratories, Inc.) were labeled with a mixture of amine-reactive activators and reporters. Alexa Fluor 405 (Invitrogen) and Cy3 (GE Healthcare) were used as the activators, and Alexa Fluor 647 (Invitrogen) was used as the reporter. Concentrations of reactive dyes were controlled such that each antibody had, on average, two activator molecules and 0.6–0.8 reporter molecules.

Imaging was done as described previously (Huang et al., 2008). In brief, STORM images were captured by a super-resolution microscope (N-STORM; Nikon) using a 100×, 1.4 NA objective lens and an EM charge-coupled device camera (iXon3 897; Andor Technology) at room temperature in a standard imaging buffer that contains 50 mM Tris, pH 7.5, 10 mM NaCl, 0.5 mg/ml glucose oxidase, 40 µg/ml catalase, 10% (wt/vol) glucose, and 0.1 M mercaptoethylamine. Two activation lasers and one imaging laser are individually shuttered and illuminate the sample in total internal reflection fluorescence mode. An objective positioner (Nano F-100; Mad City Labs Inc.) was used to stabilize the focusing of the microscope. For two-color imaging, a similar repetitive sequence of activation imaging (1 frame of activation followed by 3 frames of imaging) was used with two activation lasers. 405-nm light from the CUBE laser (Coherent) was used to activate the A405-A647 pair, and 561-nm light from a solid state laser (SAPPHIRE; Coherent) was used to activate the Cy3-A647 pair. A 647-nm laser from the CrystaLaser (DL647-100) was used for imaging. The localizations were later color-coded based on whether the A647 emission was detected after the 405-nm or 561-nm activation light. Typical laser powers used for STORM imaging were 60 mW for the imaging laser and ∼2 µW–5 µW for each of the activation lasers. A typical STORM image cycle was repeated ∼15,000–20,000 times until eventually fluorescence bleached. We used NIS-Elements software (Nikon) for correction of image drift and cross-talk statistically. For two-color STORM images, each localization was assigned as one point in the STORM image and was false-colored according to the color of the activation laser pulse.

Electrophysiology

Cultured hippocampal neurons were transfected with sh-IgSF9b (DIV 15–20), and interneuron-shaped cells, as defined by morphology (Benson et al., 1994), were whole-cell voltage-clamped at −60 mV using an Axopatch 200B amplifier (Molecular Devices). To ensure that morphologically identified cells were GABAergic interneurons, we marked cells with biocytin infusion followed by GAD67 staining, and found that ∼93% of the cells were GAD67-positive (n = 15). The extracellular solution contained (in mM): 145 NaCl, 2.5 KCl, 10 Hepes, 1.25 NaH_2PO_4, 2 $CaCl_2$, 1 $MgCl_2$, 10 glucose, and 0.4 sodium ascorbate. For mIPSC, the intracellular solution contained (in mM): 135 KCl, 10 Hepes, 8 NaCl, 4 Mg-ATP, 0.3 Na-GTP, and 0.5 EGTA. For mEPSC, the intracellular solution contained (in mM): 100 K-gluconate, 20 KCl, 10 Hepes, 8 NaCl, 4 Mg-ATP, 0.3 Na-GTP, and 0.5 EGTA. During measurement, 1 µM TTX, 50 µM AP5, and 10 µM NBQX (all from Tocris Bioscience) for mIPSC or TTX and bicuculline (10 µM; Tocris) for mEPSC were added into the extracellular solution. Synaptic currents were analyzed using a custom-written macro in Igor Pro (WaveMetrics).

Online supplemental material

Fig. S1 shows amino acid sequence alignment of IgSF9b and Dasm1/IgSF9, and generation and characterization of IgSF9b antibodies. Fig. S2 shows distribution of IgSF9b mRNAs revealed by three independent in situ hybridization probes, and gradually increasing levels of IgSF9b proteins in cultured hippocampal neurons. Fig. S3 shows that IgSF9b-expressing HEK293T cells induce clustering of IgSF9b in contacting neurites of cocultured GAD67-positive interneurons and GAD67-negative pyramidal neurons, but do not induce clustering of VGAT or vGlut1 in contacting axons or dendritic clustering of gephyrin in interneurons or in pyramidal neurons. Fig. S4 shows characterization of IgSF9b knockdown constructs,

and IgSF9b knockdown in cultured pyramidal neurons. Fig. S5 shows that S-SCAM localizes to inhibitory and excitatory synapses in interneurons. Online supplemental material is available at http://www.jcb.org/cgi/content/full/jcb.201209132/DC1. Additional data are available in the JCB DataViewer at http://dx.doi.org/10.1083/jcb.201209132.dv.

We thank Xiling Zhou for expert assistance with neuron cultures.

This work was supported by the National Research Foundation of Korea (2011-0028337 to J. Ko), a TJ Park Junior Faculty Fellowship, the POSCO TJ Park Foundation (to J. Ko), the National Research Foundation of Korea (2012K001131 to H. Kim), the Biomembrane Plasticity Research Center, the National Research Foundation of Korea (no. 20100029395 to S. Chang), the Basic Research Promotion Fund, the National Research Foundation of Korea (313-2008-2-C00690; to S. Chang), National Institutes of Health grant MH70860 and Canada Research Chair awards (to A.M. Craig), a NARSAD Young Investigator award (to H. Takahashi), a fellowship of the Alexander von Humboldt Foundation and a Marie Curie International Reintegration Grant of the European Commission (to D. Krueger), and the Institute for Basic Science in Korea (to E. Kim).

Submitted: 25 September 2012
Accepted: 25 April 2013

References

Al-Anzi, B., and R.J. Wyman. 2009. The *Drosophila* immunoglobulin gene turtle encodes guidance molecules involved in axon pathfinding. *Neural Dev.* 4:31. http://dx.doi.org/10.1186/1749-8104-4-31

Bates, M., B. Huang, G.T. Dempsey, and X. Zhuang. 2007. Multicolor super-resolution imaging with photo-switchable fluorescent probes. *Science*. 317:1749–1753. http://dx.doi.org/10.1126/science.1146598

Baude, A., Z. Nusser, J.D. Roberts, E. Mulvihill, R.A. McIlhinney, and P. Somogyi. 1993. The metabotropic glutamate receptor (mGluR1 alpha) is concentrated at perisynaptic membrane of neuronal subpopulations as detected by immunogold reaction. *Neuron*. 11:771–787. http://dx.doi.org/10.1016/0896-6273(93)90086-7

Benson, D.L., F.H. Watkins, O. Steward, and G. Banker. 1994. Characterization of GABAergic neurons in hippocampal cell cultures. *J. Neurocytol.* 23:279–295. http://dx.doi.org/10.1007/BF01188497

Biederer, T., and P. Scheiffele. 2007. Mixed-culture assays for analyzing neuronal synapse formation. *Nat. Protoc.* 2:670–676. http://dx.doi.org/10.1038/nprot.2007.92

Biederer, T., and M. Stagi. 2008. Signaling by synaptogenic molecules. *Curr. Opin. Neurobiol.* 18:261–269. http://dx.doi.org/10.1016/j.conb.2008.07.014

Blanpied, T.A., D.B. Scott, and M.D. Ehlers. 2002. Dynamics and regulation of clathrin coats at specialized endocytic zones of dendrites and spines. *Neuron*. 36:435–449. http://dx.doi.org/10.1016/S0896-6273(02)00979-0

Blundell, J., K. Tabuchi, M.F. Bolliger, C.A. Blaiss, N. Brose, X. Liu, T.C. Südhof, and C.M. Powell. 2009. Increased anxiety-like behavior in mice lacking the inhibitory synapse cell adhesion molecule neuroligin 2. *Genes Brain Behav.* 8:114–126. http://dx.doi.org/10.1111/j.1601-183X.2008.00455.x

Brose, N. 2009. Synaptogenic proteins and synaptic organizers: "many hands make light work." *Neuron*. 61:650–652. http://dx.doi.org/10.1016/j.neuron.2009.02.014

Carlin, R.K., D.J. Grab, R.S. Cohen, and P. Siekevitz. 1980. Isolation and characterization of postsynaptic densities from various brain regions: enrichment of different types of postsynaptic densities. *J. Cell Biol.* 86:831–845. http://dx.doi.org/10.1083/jcb.86.3.831

Chen, X., C. Winters, R. Azzam, X. Li, J.A. Galbraith, R.D. Leapman, and T.S. Reese. 2008. Organization of the core structure of the postsynaptic density. *Proc. Natl. Acad. Sci. USA*. 105:4453–4458. http://dx.doi.org/10.1073/pnas.0800897105

Chih, B., H. Engelman, and P. Scheiffele. 2005. Control of excitatory and inhibitory synapse formation by neuroligins. *Science*. 307:1324–1328. http://dx.doi.org/10.1126/science.1107470

Choi, J., J. Ko, E. Park, J.R. Lee, J. Yoon, S. Lim, and E. Kim. 2002. Phosphorylation of stargazin by protein kinase A regulates its interaction with PSD-95. *J. Biol. Chem.* 277:12359–12363. http://dx.doi.org/10.1074/jbc.M200528200

Choi, S., J. Ko, J.R. Lee, H.W. Lee, K. Kim, H.S. Chung, H. Kim, and E. Kim. 2006. ARF6 and EFA6A regulate the development and maintenance of dendritic spines. *J. Neurosci.* 26:4811–4819. http://dx.doi.org/10.1523/JNEUROSCI.4182-05.2006

Chubykin, A.A., D. Atasoy, M.R. Etherton, N. Brose, E.T. Kavalali, J.R. Gibson, and T.C. Südhof. 2007. Activity-dependent validation of excitatory versus inhibitory synapses by neuroligin-1 versus neuroligin-2. *Neuron*. 54:919–931. http://dx.doi.org/10.1016/j.neuron.2007.05.029

Craig, A.M., and Y. Kang. 2007. Neurexin-neuroligin signaling in synapse development. *Curr. Opin. Neurobiol.* 17:43–52. http://dx.doi.org/10.1016/j.conb.2007.01.011

Dalva, M.B., A.C. McClelland, and M.S. Kayser. 2007. Cell adhesion molecules: signalling functions at the synapse. *Nat. Rev. Neurosci.* 8:206–220. http://dx.doi.org/10.1038/nrn2075

Dani, A., B. Huang, J. Bergan, C. Dulac, and X. Zhuang. 2010. Superresolution imaging of chemical synapses in the brain. *Neuron*. 68:843–856. http://dx.doi.org/10.1016/j.neuron.2010.11.021

Dobie, F.A., and A.M. Craig. 2011. Inhibitory synapse dynamics: coordinated presynaptic and postsynaptic mobility and the major contribution of recycled vesicles to new synapse formation. *J. Neurosci.* 31:10481–10493. http://dx.doi.org/10.1523/JNEUROSCI.6023-10.2011

Doudney, K., J.N. Murdoch, C. Braybrook, C. Paternotte, L. Bentley, A.J. Copp, and P. Stanier. 2002. Cloning and characterization of Igsf9 in mouse and human: a new member of the immunoglobulin superfamily expressed in the developing nervous system. *Genomics*. 79:663–670. http://dx.doi.org/10.1006/geno.2002.6757

Ferguson, K., H. Long, S. Cameron, W.T. Chang, and Y. Rao. 2009. The conserved Ig superfamily member Turtle mediates axonal tiling in *Drosophila*. *J. Neurosci.* 29:14151–14159. http://dx.doi.org/10.1523/JNEUROSCI.2497-09.2009

Fritschy, J.M., R.J. Harvey, and G. Schwarz. 2008. Gephyrin: where do we stand, where do we go? *Trends Neurosci.* 31:257–264. http://dx.doi.org/10.1016/j.tins.2008.02.006

Fritschy, J.M., P. Panzanelli, and S.K. Tyagarajan. 2012. Molecular and functional heterogeneity of GABAergic synapses. *Cell. Mol. Life Sci.* 69:2485–2499. http://dx.doi.org/10.1007/s00018-012-0926-4

Fukaya, M., A. Kamata, Y. Hara, H. Tamaki, O. Katsumata, N. Ito, S. Takeda, Y. Hata, T. Suzuki, M. Watanabe, et al. 2011. SynArfGEF is a guanine nucleotide exchange factor for Arf6 and localizes preferentially at postsynaptic specializations of inhibitory synapses. *J. Neurochem.* 116:1122–1137. http://dx.doi.org/10.1111/j.1471-4159.2010.07167.x

Gerrow, K., S. Romorini, S.M. Nabi, M.A. Colicos, C. Sala, and A. El-Husseini. 2006. A preformed complex of postsynaptic proteins is involved in excitatory synapse development. *Neuron*. 49:547–562. http://dx.doi.org/10.1016/j.neuron.2006.01.015

Gibson, J.R., K.M. Huber, and T.C. Südhof. 2009. Neuroligin-2 deletion selectively decreases inhibitory synaptic transmission originating from fast-spiking but not from somatostatin-positive interneurons. *J. Neurosci.* 29:13883–13897. http://dx.doi.org/10.1523/JNEUROSCI.2457-09.2009

Goslin, K., and G. Banker. 1991. Rat hippocampal neurons in low-density culture. *In* Culturing Nerve Cells. G. Banker and K. Goslin, editors. The MIT Press, Cambridge, MA. 337–370.

Graf, E.R., X. Zhang, S.X. Jin, M.W. Linhoff, and A.M. Craig. 2004. Neurexins induce differentiation of GABA and glutamate postsynaptic specializations via neuroligins. *Cell*. 119:1013–1026. http://dx.doi.org/10.1016/j.cell.2004.11.035

Graf, E.R., Y. Kang, A.M. Hauner, and A.M. Craig. 2006. Structure function and splice site analysis of the synaptogenic activity of the neurexin-1 beta LNS domain. *J. Neurosci.* 26:4256–4265. http://dx.doi.org/10.1523/JNEUROSCI.1253-05.2006

Hirao, K., Y. Hata, N. Ide, M. Takeuchi, M. Irie, I. Yao, M. Deguchi, A. Toyoda, T.C. Sudhof, and Y. Takai. 1998. A novel multiple PDZ domain-containing molecule interacting with N-methyl-D-aspartate receptors and neuronal cell adhesion proteins. *J. Biol. Chem.* 273:21105–21110. http://dx.doi.org/10.1074/jbc.273.33.21105

Hoon, M., G. Bauer, J.M. Fritschy, T. Moser, B.H. Falkenburger, and F. Varoqueaux. 2009. Neuroligin 2 controls the maturation of GABAergic synapses and information processing in the retina. *J. Neurosci.* 29:8039–8050. http://dx.doi.org/10.1523/JNEUROSCI.0534-09.2009

Huang, B., W. Wang, M. Bates, and X. Zhuang. 2008. Three-dimensional super-resolution imaging by stochastic optical reconstruction microscopy. *Science*. 319:810–813. http://dx.doi.org/10.1126/science.1153529

Huttner, W.B., W. Schiebler, P. Greengard, and P. De Camilli. 1983. Synapsin I (protein I), a nerve terminal-specific phosphoprotein. III. Its association with synaptic vesicles studied in a highly purified synaptic vesicle preparation. *J. Cell Biol.* 96:1374–1388. http://dx.doi.org/10.1083/jcb.96.5.1374

Irie, M., Y. Hata, M. Takeuchi, K. Ichtchenko, A. Toyoda, K. Hirao, Y. Takai, T.W. Rosahl, and T.C. Südhof. 1997. Binding of neuroligins to PSD-95. *Science*. 277:1511–1515. http://dx.doi.org/10.1126/science.277.5331.1511

Jedlicka, P., M. Hoon, T. Papadopoulos, A. Vlachos, R. Winkels, A. Poulopoulos, H. Betz, T. Deller, N. Brose, F. Varoqueaux, and S.W.

Schwarzacher. 2011. Increased dentate gyrus excitability in neuroligin-2-deficient mice in vivo. *Cereb. Cortex*. 21:357–367. http://dx.doi.org/10.1093/cercor/bhq100

Johnson-Venkatesh, E.M., and H. Umemori. 2010. Secreted factors as synaptic organizers. *Eur. J. Neurosci.* 32:181–190. http://dx.doi.org/10.1111/j.1460-9568.2010.07338.x

Kim, E., and M. Sheng. 2004. PDZ domain proteins of synapses. *Nat. Rev. Neurosci.* 5:771–781. http://dx.doi.org/10.1038/nrn1517

Kim, D., E.H. Kim, C. Kim, W. Sun, H.J. Kim, C.S. Uhm, S.H. Park, and H. Kim. 2003. Differential regulation of metallothionein-I, II, and III mRNA expression in the rat brain following kainic acid treatment. *Neuroreport*. 14:679–682. http://dx.doi.org/10.1097/00001756-200304150-00004

Kim, S., A. Burette, H.S. Chung, S.K. Kwon, J. Woo, H.W. Lee, K. Kim, H. Kim, R.J. Weinberg, and E. Kim. 2006. NGL family PSD-95-interacting adhesion molecules regulate excitatory synapse formation. *Nat. Neurosci.* 9:1294–1301. http://dx.doi.org/10.1038/nn1763

Kim, M.H., J. Choi, J. Yang, W. Chung, J.H. Kim, S.K. Paik, K. Kim, S. Han, H. Won, Y.S. Bae, et al. 2009. Enhanced NMDA receptor-mediated synaptic transmission, enhanced long-term potentiation, and impaired learning and memory in mice lacking IRSp53. *J. Neurosci.* 29:1586–1595. http://dx.doi.org/10.1523/JNEUROSCI.4306-08.2009

Ko, J., M.V. Fuccillo, R.C. Malenka, and T.C. Südhof. 2009. LRRTM2 functions as a neurexin ligand in promoting excitatory synapse formation. *Neuron*. 64:791–798. http://dx.doi.org/10.1016/j.neuron.2009.12.012

Krueger, D.D., L.P. Tuffy, T. Papadopoulos, and N. Brose. 2012. The role of neurexins and neuroligins in the formation, maturation, and function of vertebrate synapses. *Curr. Opin. Neurobiol.* 22:412–422. http://dx.doi.org/10.1016/j.conb.2012.02.012

Lévi, S., R.M. Grady, M.D. Henry, K.P. Campbell, J.R. Sanes, and A.M. Craig. 2002. Dystroglycan is selectively associated with inhibitory GABAergic synapses but is dispensable for their differentiation. *J. Neurosci.* 22 :4274–4285.

Levinson, J.N., N. Chéry, K. Huang, T.P. Wong, K. Gerrow, R. Kang, O. Prange, Y.T. Wang, and A. El-Husseini. 2005. Neuroligins mediate excitatory and inhibitory synapse formation: involvement of PSD-95 and neurexin-1beta in neuroligin-induced synaptic specificity. *J. Biol. Chem.* 280:17312–17319. http://dx.doi.org/10.1074/jbc.M413812200

Lim, S., C. Sala, J. Yoon, S. Park, S. Kuroda, M. Sheng, and E. Kim. 2001. Sharpin, a novel postsynaptic density protein that directly interacts with the shank family of proteins. *Mol. Cell. Neurosci.* 17:385–397. http://dx.doi.org/10.1006/mcne.2000.0940

Long, H., Y. Ou, Y. Rao, and D.J. van Meyel. 2009. Dendrite branching and self-avoidance are controlled by Turtle, a conserved IgSF protein in *Drosophila*. *Development*. 136:3475–3484. http://dx.doi.org/10.1242/dev.040220

Lu, J., T.D. Helton, T.A. Blanpied, B. Rácz, T.M. Newpher, R.J. Weinberg, and M.D. Ehlers. 2007. Postsynaptic positioning of endocytic zones and AMPA receptor cycling by physical coupling of dynamin-3 to Homer. *Neuron*. 55:874–889. http://dx.doi.org/10.1016/j.neuron.2007.06.041

Luscher, B., T. Fuchs, and C.L. Kilpatrick. 2011. GABAA receptor trafficking-mediated plasticity of inhibitory synapses. *Neuron*. 70:385–409. http://dx.doi.org/10.1016/j.neuron.2011.03.024

Marshall, C.R., E.J. Young, A.M. Pani, M.L. Freckmann, Y. Lacassie, C. Howald, K.K. Fitzgerald, M. Peippo, C.A. Morris, K. Shane, et al. 2008. Infantile spasms is associated with deletion of the MAGI2 gene on chromosome 7q11.23-q21.11. *Am. J. Hum. Genet.* 83:106–111. http://dx.doi.org/10.1016/j.ajhg.2008.06.001

Mishra, A., B. Knerr, S. Paixão, E.R. Kramer, and R. Klein. 2008. The protein dendrite arborization and synapse maturation 1 (Dasm-1) is dispensable for dendrite arborization. *Mol. Cell. Biol.* 28:2782–2791. http://dx.doi.org/10.1128/MCB.02102-07

Mok, H., H. Shin, S. Kim, J.R. Lee, J. Yoon, and E. Kim. 2002. Association of the kinesin superfamily motor protein KIF1Balpha with postsynaptic density-95 (PSD-95), synapse-associated protein-97, and synaptic scaffolding molecule PSD-95/discs large/zona occludens-1 proteins. *J. Neurosci.* 22:5253–5258.

Poulopoulos, A., G. Aramuni, G. Meyer, T. Soykan, M. Hoon, T. Papadopoulos, M. Zhang, I. Paarmann, C. Fuchs, K. Harvey, et al. 2009. Neuroligin 2 drives postsynaptic assembly at perisomatic inhibitory synapses through gephyrin and collybistin. *Neuron*. 63:628–642. http://dx.doi.org/10.1016/j.neuron.2009.08.023

Scheiffele, P., J. Fan, J. Choih, R. Fetter, and T. Serafini. 2000. Neuroligin expressed in nonneuronal cells triggers presynaptic development in contacting axons. *Cell*. 101:657–669. http://dx.doi.org/10.1016/S0092-8674(00)80877-6

Shapira, M., R.G. Zhai, T. Dresbach, T. Bresler, V.I. Torres, E.D. Gundelfinger, N.E. Ziv, and C.C. Garner. 2003. Unitary assembly of presynaptic active zones from Piccolo-Bassoon transport vesicles. *Neuron*. 38:237–252. http://dx.doi.org/10.1016/S0896-6273(03)00207-1

Shen, K., and P. Scheiffele. 2010. Genetics and cell biology of building specific synaptic connectivity. *Annu. Rev. Neurosci.* 33:473–507. http://dx.doi.org/10.1146/annurev.neuro.051508.135302

Sheng, M., and E. Kim. 2011. The postsynaptic organization of synapses. *Cold Spring Harb. Perspect. Biol.* 3:a005678. http://dx.doi.org/10.1101/cshperspect.a005678

Shi, S.H., T. Cheng, L.Y. Jan, and Y.N. Jan. 2004a. The immunoglobulin family member dendrite arborization and synapse maturation 1 (Dasm1) controls excitatory synapse maturation. *Proc. Natl. Acad. Sci. USA*. 101:13346–13351. http://dx.doi.org/10.1073/pnas.0405371101

Shi, S.H., D.N. Cox, D. Wang, L.Y. Jan, and Y.N. Jan. 2004b. Control of dendrite arborization by an Ig family member, dendrite arborization and synapse maturation 1 (Dasm1). *Proc. Natl. Acad. Sci. USA*. 101:13341–13345. http://dx.doi.org/10.1073/pnas.0405370101

Shyn, S.I., J. Shi, J.B. Kraft, J.B. Potash, J.A. Knowles, M.M. Weissman, H.A. Garriock, J.S. Yokoyama, P.J. McGrath, E.J. Peters, et al. 2011. Novel loci for major depression identified by genome-wide association study of Sequenced Treatment Alternatives to Relieve Depression and meta-analysis of three studies. *Mol. Psychiatry*. 16:202–215. http://dx.doi.org/10.1038/mp.2009.125

Siddiqui, T.J., and A.M. Craig. 2011. Synaptic organizing complexes. *Curr. Opin. Neurobiol.* 21:132–143. http://dx.doi.org/10.1016/j.conb.2010.08.016

Südhof, T.C. 2008. Neuroligins and neurexins link synaptic function to cognitive disease. *Nature*. 455:903–911. http://dx.doi.org/10.1038/nature07456

Sumita, K., Y. Sato, J. Iida, A. Kawata, M. Hamano, S. Hirabayashi, K. Ohno, E. Peles, and Y. Hata. 2007. Synaptic scaffolding molecule (S-SCAM) membrane-associated guanylate kinase with inverted organization (MAGI)-2 is associated with cell adhesion molecules at inhibitory synapses in rat hippocampal neurons. *J. Neurochem.* 100:154–166. http://dx.doi.org/10.1111/j.1471-4159.2006.04170.x

Takahashi, H., P. Arstikaitis, T. Prasad, T.E. Bartlett, Y.T. Wang, T.H. Murphy, and A.M. Craig. 2011. Postsynaptic TrkC and presynaptic PTPσ function as a bidirectional excitatory synaptic organizing complex. *Neuron*. 69:287–303. http://dx.doi.org/10.1016/j.neuron.2010.12.024

Takahashi, H., K. Katayama, K. Sohya, H. Miyamoto, T. Prasad, Y. Matsumoto, M. Ota, H. Yasuda, T. Tsumoto, J. Aruga, and A.M. Craig. 2012. Selective control of inhibitory synapse development by Slitrk3-PTPδ trans-synaptic interaction. *Nat. Neurosci.* 15:389–398: S1–S2. http://dx.doi.org/10.1038/nn.3040

Tallafuss, A., J.R. Constable, and P. Washbourne. 2010. Organization of central synapses by adhesion molecules. *Eur. J. Neurosci.* 32:198–206. http://dx.doi.org/10.1111/j.1460-9568.2010.07340.x

Tyagarajan, S.K., and J.M. Fritschy. 2010. GABA(A) receptors, gephyrin and homeostatic synaptic plasticity. *J. Physiol.* 588:101–106. http://dx.doi.org/10.1113/jphysiol.2009.178517

Uchida, N., Y. Honjo, K.R. Johnson, M.J. Wheelock, and M. Takeichi. 1996. The catenin/cadherin adhesion system is localized in synaptic junctions bordering transmitter release zones. *J. Cell Biol.* 135:767–779. http://dx.doi.org/10.1083/jcb.135.3.767

Varoqueaux, F., S. Jamain, and N. Brose. 2004. Neuroligin 2 is exclusively localized to inhibitory synapses. *Eur. J. Cell Biol.* 83:449–456. http://dx.doi.org/10.1078/0171-9335-00410

Varoqueaux, F., G. Aramuni, R.L. Rawson, R. Mohrmann, M. Missler, K. Gottmann, W. Zhang, T.C. Südhof, and N. Brose. 2006. Neuroligins determine synapse maturation and function. *Neuron*. 51:741–754. http://dx.doi.org/10.1016/j.neuron.2006.09.003

Williams, M.E., J. de Wit, and A. Ghosh. 2010. Molecular mechanisms of synaptic specificity in developing neural circuits. *Neuron*. 68:9–18. http://dx.doi.org/10.1016/j.neuron.2010.09.007

Woo, J., S.K. Kwon, and E. Kim. 2009. The NGL family of leucine-rich repeat-containing synaptic adhesion molecules. *Mol. Cell. Neurosci.* 42:1–10. http://dx.doi.org/10.1016/j.mcn.2009.05.008

Yuzaki, M. 2010. Synapse formation and maintenance by C1q family proteins: a new class of secreted synapse organizers. *Eur. J. Neurosci.* 32:191–197. http://dx.doi.org/10.1111/j.1460-9568.2010.07346.x

Zhai, R.G., H. Vardinon-Friedman, C. Cases-Langhoff, B. Becker, E.D. Gundelfinger, N.E. Ziv, and C.C. Garner. 2001. Assembling the presynaptic active zone: a characterization of an active one precursor vesicle. *Neuron*. 29:131–143. http://dx.doi.org/10.1016/S0896-6273(01)00185-4